A Comparison of Generative Design with Experimental Data for a Bike Frame

A thesis submitted by:
Matias A. Aranguiz

IN PARTIAL FULFILMENT OF THE REQUIREMENTS FOR THE DEGREE OF

MASTER OF SCIENCE

In

MECHANICAL ENGINEERING

Tufts University

May 2023

2023, Matias A. Aranguiz

Adviser: Chris Rogers

Abstract

This thesis investigates the potential of generative design software to create optimal part designs based on specific requirements, as well as its limitations and challenges. The study involved running 20 generative design models, showcasing some of them in the research, 3D-printing three models, and testing them on an Instron machine. The results revealed that the software can accurately simulate real-world loads under certain conditions, with one model showing agreement within 1%. However, the other models were off by 36.6% and 51.9%, indicating the need to predict and control external factors to achieve reliable results. Additionally, creating a lightweight bike frame capable of carrying more weight than a typical frame requires a powerful computer and a complex process. Overall, this research contributes to the understanding of the potential of generative design and highlights the challenges that need to be addressed to fully realize its benefits.

Acknowledgments

Completing this study could not have been possible without the help of Dr. Chris Rogers and Dr. Gary Leisk, who not only guided me in this study for my master's degree but also played a prominent role in my undergraduate education.

I also want to thank Dr. Matthew Mueller and PTC, who was kind enough to allow me to use the Creo Parametric generative design software. Additionally, I was allowed to talk with a design engineer who uses generative design for the company and ask many helpful questions.

Table of Contents

List of Figures

Chapter 1: Introduction

With the evolution of new additive manufacturing techniques, most commonly the ability to use 3D printers with various materials, companies can consider more complex shapes. Parts usually considered extremely difficult to manufacture are now a possibility and are paving the way for implementing more modern Computer-Aided Design (CAD) methods. One of these methods is called Generative Design (GD), an algorithm that attempts to optimize CAD models while maintaining the engineering requirements of the specified part presented by the designer.

1.1   Computer-Aided Design

Computer-Aided design is said to have been created after Computer-Aided Manufacturing (CAM) [1]. CAM originally involved the insertion of paper tapes with numerical data into machines [1]. The paper tapes would eventually develop into what today we call G-Code. The machines utilized this data to position and direct tools to manufacture the item needed in production. The first CAM software program is accredited to Dr. Patrick J. Hanratty for the development of a numerical control (NC) programming tool called PRONTO [1]. Since then, CAD and CAM have evolved substantially from wire-frame modeling to surface modeling and are currently at a feature-based parametric modeling stage. Since the 1960s, CAD technologies have started finding their way into colleges and universities for students in different fields to learn [2]. Today, CAD is so widely used that users can be separated into different groups. These groups are: *CAD Users* – who utilize CAD tools in their day-to-day jobs, *CAD application developers* – who develop CAD packages using Application Programming Interfaces (APIs)

provided by software vendors, *CAD Software Developers* – who are directly involved as staff in researching and developing CAD software, *CAD Managers* – who can manage one or multiple of the aforementioned groups, and simply *Others* – who are involved in the interactions/usage of CAD software but do not specifically fit in the other categories [2].

1.2   The Rise of Generative Design

It may seem that generative design is a new technology that only has been around for a couple of years. However, "the term 'Generative Design' has been around for many decades. The idea is straightforward, a parametric model that evaluates the outcome against some design goal and automatically re-runs until the design goal(s) is achieved or optimized" [3]. Note that the parameters are slightly changed before the simulation is re-ran. Since the first integrated circuit was created in 1958, computers' computational speed and memory capacity have grown exponentially (Moore's Law) [4]. Although the idea was around for decades, it was not until recently that computers were powerful and cheap enough to run all these calculations in a reasonable amount of time, ranging from only a couple minutes to some hours. Subtractive manufacturing was, and still is, the main form of manufacturing along with molding and casting. However, 3D printing has developed and become widespread enough to allow the consideration of generative design during the CAD modeling process.

Why replace current design methods in CAD software for this new optimization method? Some key ideas are performance, price, and the environment. Performance can be demonstrated in the Czinger 21C Hypercar structure. As described:

> …a mix of computational engineering and generative design, using a computer to optimize parts for a given purpose within a set of constraints. Such constraints include things like weight, strength, size, material, and mounting points. They would be subsequently input into the computer, and it would return the lightest, strongest part

based on the given constraints by figuring out exactly where material does and does not need to be. [5]

Price benefits are reflected in the material required to create a part. Generative design and topology optimization provide part options as light as possible under the given conditions. This means there will not be any unnecessary material used in the part, and if done appropriately with 3D printers, reduce the overall cost of making the part. It is important to remember the process is more complex so the longer runtimes may make it more expensive in that front. Claudius Peters, an industrial machinery manufacturer for materials handling and processing, is working on a new clinker cooler (a device used in the production of cement to cool and solidify hot clinker from the kiln), estimated to save thousands of euros on each one produced due to the material saving [6]. The parts presented to the designer would be too difficult to manufacture in typical subtractive manufacturing techniques. Even if modified to be possible, the original solid block, bar, metal, or other material will most likely still have scrapped leftovers.

Perhaps the most important effect generative design can have is on the environment. Airbus used generative design to redesign a partition in their A320 aircraft. This partition's weight was reduced by 45 percent. According to an estimation by Airbus, that partition on an A320 would reduce carbon emissions by 465,000 tons per year [6]. Generative design is also widely used in designing new buildings. It was shown that using a generative design method, a tall building in the city of Toronto could have a 31% larger ARCH score with 7% less EE than one compared to in a case study [7]. EE stands for Embedded Emissions of the building, which are product and construction stages emissions. 7% less corresponded to 1 $GgCO_{2\text{-eq}}$ (1 billion grams of greenhouse gas emissions, measured in terms of their carbon dioxide equivalent). ARCH represents the architectural score of the building, which give a numerical representation

to the aesthetics and site views of a building [7]. The larger this score, the more desirable the building.

With generative design being relatively new in the engineering manufacturing field, there are very few resources on the web to attempt to learn it, and no courses are being offered or touching on, at least yet, generative design at Tufts University and likely many other schools as well. Testing actual experimental data and comparing it with the computer's expected FEA analysis will prove valuable and give detail about the current state of the software.

1.3 Contributions

In this thesis, I present an investigation and demonstration of the capabilities of one of these new Generative Design programs. Specifically, Generative Design as provided in PTC's Creo version 9.0.0.0. I created a realistic scaled-down prototype of a bike frame optimized by generative design and topology optimization. I commented on the learning process and computational power for the utilized software. I demonstrated through Finite Element Analysis (FEA) after the studies that the frames scaled down by 5 should not yield under the provided forces. Lastly, I physically tested on an Instron machine the models to determine the force/displacement plots to compare with the provided computational data. I want this to serve as a future resource for students as an initial experience and demonstration of generative design so they can use it to create their parts and help prepare for challenges that may be encountered.

Chapter 2: Background

2.1 Traditional Design Optimization

Traditionally, designers would follow a specific method and iterate on it many times. The more simple case starts with a part or structural component that has been previously designed. If an old structural component has had failures in the field, it is easy to locate problems and attempt to iterate to fix the cause of the failure. However, if the old design performs well in the field, there is no way to know if the component is overdesigned [8]. As these components become more complex, the designer's task to devise optimal parts becomes much more difficult. Also, if the basic architecture of the new component design is far from optimum, the designer can spend a lot of time trying to improve on this starting point [8].

In this method (as shown in figure 1), one begins by defining the constraints of the wanted part. This includes determining the forces or loads that will be experienced by the part, determining where the physical constraints and connections are for the part, and going through a material selection process. Users can specify not only forces but also moments, pressures, temperatures, preloads, gravity, and maybe even some more complex ones, such as centrifugal effects [9]. These are, for example, some of the types of structure loads offered in Creo. Constraints define the extent to which a model can move in reference to a coordinate system and, along with the loads, provide the software of choice with the real-world conditions that it uses as the basis for analysis [10]. Providing the inaccurate loads and constraints can cause a computer program to perform faulty stress calculations so it is critical to provide accurate conditions.

Constraints are categorized into constraint sets: Displacement constraints, Symmetry constraints, and Planar, Pin, and Ball Constraints [10].
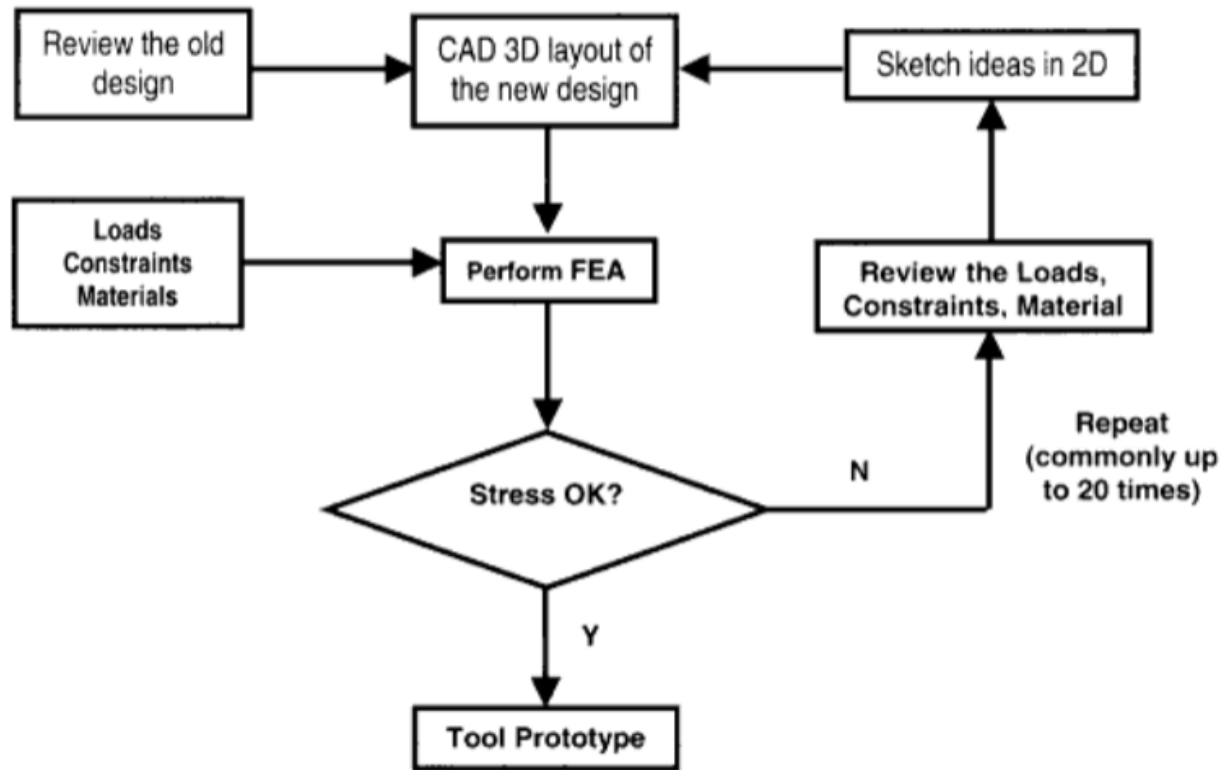
Figure 1: A traditional Design Method Flow Chart for a simulation based design approach that can be followed to optimize a part without topology optimization or generative design [8]

Sketching is one of the main differences between the traditional optimization method of a part and the utilization of Artificial Intelligence (AI) to come up with the part. In traditional methods, sketching is widely used since the method starts with what is known about current parts and the application data for the new component. This information is combined with the designer's ideas and personal insight of the component requirements to generate 2D sketches of the design [8]. Sketching is so vital that full studies have been done on how it affects the design process. Sketching facilitates the transition from general descriptive knowledge into specific depiction. Designers sketch "…to foresee the results of the synthesis or manipulation of objects

without actually executing such operations" [11]. The importance is that although sketches are vital in current design processes, the more advanced AI software becomes, the less they will be needed.

2.1.1 Finite Element Analysis (FEA)

At the center of the optimization process (see figure 1) is a key step that remains even after the introduction of AI. "Perform FEA," or Finite Element Analysis, is the key to optimizing a part, at least in terms of stress optimization. Finite element analysis is a numerical method that originated as a way to perform stress analysis in aircraft; Today, it is used in solid mechanics, fluid flow, heat transfer, electric and magnetic fields, and other fields [12].

2.1.2 A General Description of FEA

Finite element analysis uses the information provided by the designer, such as a 3D CAD model, loads, constraints, and materials (see figure 1), to attempt and predict the behavior of the entire structure. The clearest example to visualize is displacements in solid mechanics problems. Displacement is a basic unknown and is also called a field variable [12]. If a continuum is used to solve for the unknowns, the number of unknowns is infinite. To solve this, FEA splits the part into a finite number of parts called elements and "expresses the unknown field variables in terms of assumed approximating functions within each element. The approximating functions are defined in terms of field variables of specified points called nodes…" [12] (see figure 2).

Once these elements and nodes are defined, each element region is assigned properties so numerical calculations can be performed on them. In the specific example being explored, one must find each element's stiffness characteristics or force-displacement [12]. This relationship

can be given mathematically in terms of an element stiffness matrix denoted by $[k]_e$, a nodal

displacement vector for the element denoted by $\{\delta\}_e$, and $\{F\}_e$ as the nodal force vector [12].
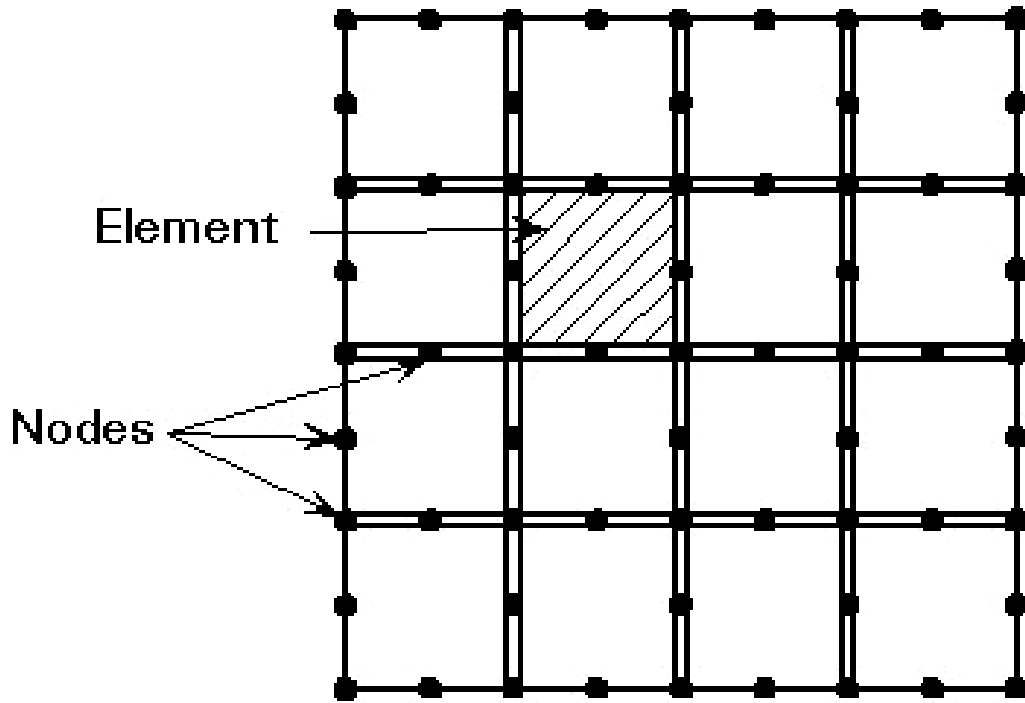
Figure 2: A visual representation of elements and nodes in a finite element method [13]

$$[k]_e \{\delta\}_e = \{F\}_e$$

Figure 3: The mathematical relationship utilized in Finite Element Analysis calculations [12]

The "element properties are afterwards used to assemble global properties/structure properties to

get system equations $[k]\{\delta\}=\{F\}$" and "then boundary conditions are imposed." The system of

equations is solved in this matrix form to get the unknowns for each node and afterward can be

used to calculate other unknown values (stressed, strains, moments, etc.) [12]. In a simplified list,

the process of finite element analysis can be expressed as follows:

(i)   "Select suitable field variables and the elements."

(ii)   "Discritise the continua."

(iii)   "Select interpolation functions."

(iv)   "Find the element properties."

(v)   "Assemble element properties to get global properties."

(vi)   "Impose the boundary conditions."

(vii)   "Solve the system equations to get the nodal unknowns."

(viii)   "Make the additional calculations to get the required values." [12]

2.2   Topology Optimization

Topology optimization is a computational technique used in engineering design to optimize the material distribution of a structure, given specific design criteria such as weight, strength, and/or stiffness. "The aim of structural optimization is to obtain an optimal design. An optimal design refers to the (locally) best solution to the optimization problem one considers" [15]. Topology optimization was proposed for the first time to deal with discrete truss structures by W. Dorn, R. Gomory, and H. Greenberg in *Automatic design of optimal structures* [16]. This was later modified and built upon to turn into density-based topology optimization, the technique used to optimize the material distribution of the structure.

2.2.1 Stress-Constrained Topology Optimization (SCT)

Ensuring that a part will last and not yield under a force is one of the leading design concerns when designing a part. Stress-constrained topology optimization is one of the foundations of generative design software. During SCT optimization, the constraint maintains the stress values, or Von Mises calculations, under the selected material's yield value while optimizing the part's material. This will return the part with the least volume and, consequently, mass, which can still hold the desired amount of force. The formulation of this optimization can

be described with a set of five equations. Although a full mathematical explanation of topology optimization will not be covered, a more detailed explanation can be found in D. Yang *et al.* [17], E. Holmberg *et al.*[18] and A. Gebisa *et al.* [19]. A line by line explanation of figures 4 and 5 is provided below.

$$
\begin{aligned}
\min_{\rho} \ c &= \tfrac{1}{2}\mathbf{f}^{\mathrm{T}}\mathbf{u} \\
\mathrm{s.t.} \quad \mathbf{Ku} &= \mathbf{f} \\
V &\leqslant \overline{V} \\
\sigma_e^{\mathrm{vM}} &\leqslant \overline{\sigma} \ (e = 1,2,\ldots NE) \\
0 &< \rho_{\min} \leqslant \rho_i \leqslant 1 \ (i = 1,2,\ldots N)
\end{aligned}
$$

Figure 4: General equation for the topology optimization to increase stiffness [17]

$$
\begin{aligned}
\min_{\rho} \ V &= \sum_{e=1}^{NE} \rho_e V_e \\
\mathrm{s.t.} \quad \mathbf{Ku} &= \mathbf{f} \\
\sigma_e^{\mathrm{vM}} &\leqslant \overline{\sigma} \ (e = 1,2,\ldots NE) \\
0 &< \rho_{\min} \leqslant \rho_i \leqslant 1 \ (i = 1,2,\ldots N)
\end{aligned}
$$

Figure 5: General equation for the topology optimization to decrease volume [17]

Looking at the topology optimization equation (see figures 4 and 5), a general description of the model can be shown. The first lines on each model indicate whether the function being minimized is volume, denoted by V, or the mean compliance of the structure, denoted by c. The second line on the equations is the same for both and is something already explored in figure 4. This is simply assigning the stiffness characteristics or force-displacement on each element. In the equation to increase stiffness, an additional term is required to set an upper bound to the

volume. This upper bound is $\overline{V}$, used to prevent the volume from becoming too large and returning a large part. This term is unnecessary during the topology optimization for volume reduction because the goal is to reduce the volume. As for the next term, define σ_e^{vM} as the "equivalent Von Mises stress of the eth element, and $\bar{\sigma}$ is the stress limit value" [17]. The index e is an integer value from 1 to the number of elements. This term will ensure that the stress experienced by each element is not greater than that limit value (which would result in the yielding of the part). The last line in the equations is utilized to prevent singularities in the stiffness matrix; otherwise, this would result in the optimization formulation having a trivial solution for zero densities [17].

$$\sigma_e^{vM} = (\sigma_e^{T} \mathbf{V} \sigma_e)^{\frac{1}{2}}$$

Figure 6: Calculation to find the von Mises stress of the eth element [17]

$$\mathbf{V} = \begin{bmatrix} 1 & -1/2 & 0 \\ -1/2 & 1 & 0 \\ 0 & 0 & 3 \end{bmatrix}$$

Figure 7: Matrix $\mathbf{V}$, constant matrix only for the plane stress case [17]

$$\sigma_e = \rho_e^s \mathbf{D}_0 \mathbf{B}^c \mathbf{u}_e$$

Figure 8: Equation to calculate the element stress vector used in the optimization equations [17]

To give a more complete description of the calculation, the von Mises stress of the eth element σ_e^{vM} is calculated by multiplying the stress vector and its transpose with the constant matrix for plane stress $\mathbf{V}$ (see figure 7) and taking the square root of the result (see figure 6). To determine this stress vector for the calculations, "$\mathbf{B}^C$ represents the strain-displacement matrix of

the element centroid, $\boldsymbol{u}_e$ means the elemental displacement vector and s is set to be a suggested value of 0.5" [17], [18]. Topology optimization can be performed on a part using these as the basis for the calculations. Again, more is covered in D. Yang *et al.* [17], E. Holmberg *et al.*[18] and A. Gebisa *et al.* [19].

2.2.2 Utilizing Topology Optimization

Topology optimization is usually initiated by giving the software program an over-designed part that can be optimized. This over-designed part can either purposely be over-designed or simply be an initial guess by the designer about what the part should look like. The topology optimization procedure can be outlined in a flowchart like the traditional design optimization process.

To use topology optimization, one must define the constraints. Much like in a traditional design optimization process, the computer must have the same parameters defined as for an FEA analysis. Utilizing these parameters, the part can undergo topology optimization with the initial part given to the software as the "limit volume." This model seems more complicated than the traditional design procedure, but the benefits of this method were demonstrated to produce better solutions in less time [8]. This is because the iteration part of the flowchart only has to be performed once with topology optimization, with the user only running the program once and the computer performing the many iterations.

Space claim of all internal parts to be enclosed

External envelope of permitted working volume

Materials Constraints Loads

Topological optimization

Preliminary shape adapted to CAD overlay

Sketched 2D concepts

CAD model as a part or in an assembly

Adapt model for analysis and perform FEA

Review assumptions for materials loads constraints

CAD 3D overlay on FEA design

Results OK?

N

Y

Shape optimization

Y

Shape optimization needed?

N

Redesign needed?

Y

N

Prototype the part

Figure 9: A topology optimization process flowchart for prototyping a part [8]
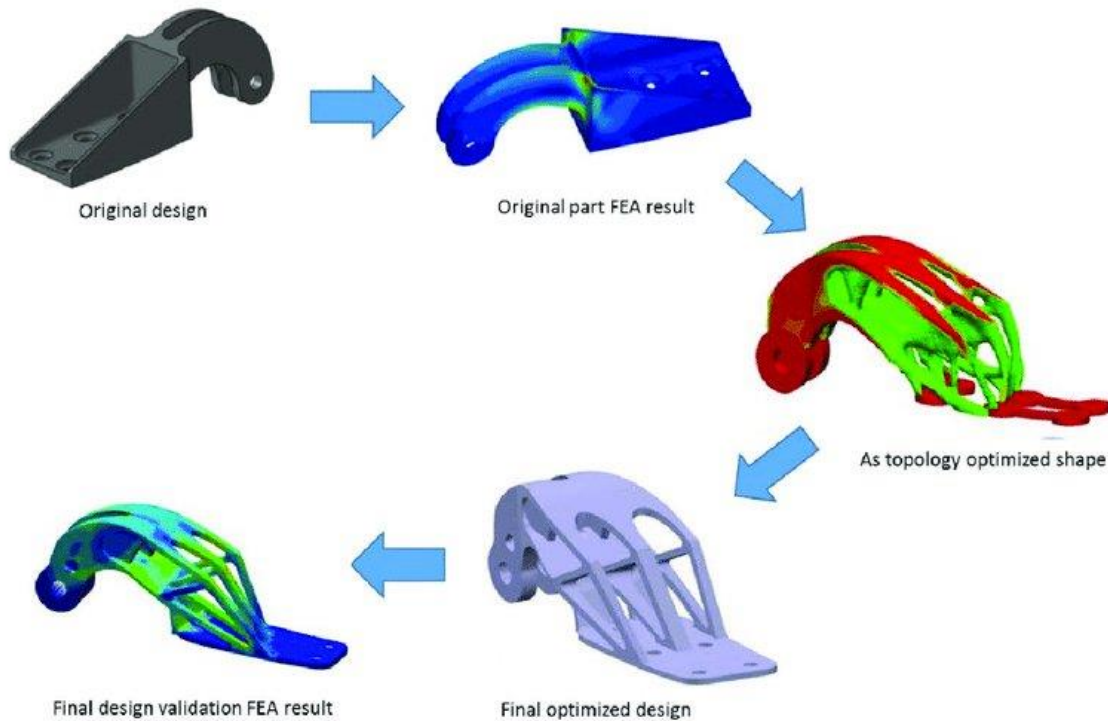
Figure 10: A topology optimization process demonstration [19]

In figure 10, we see a demonstration of the optimization process a designer would go through. The original design is the "over-designed" part, typically considered a final result in the traditional design engineering process. An initial FEA is performed to confirm that this part would not yield. If the original part yields, it is difficult for topology optimization to converge to a part since the overall goal is to remove volume and not add it. Topology optimization can add more volume to a part if it was removed initially during the process; recall that the initial part will serve as the limit volume for the process. In figure 10, two of the steps are FEA results steps 2 and 5). Step 2 is the original FEA calculation with a color gradient that follows blue to green to red, with blue representing low von Mises stress calculations compared to the yielding point of the material selected and red being high. For most of the part, the stress is very low, indicative of an excess of material in those regions. More material or a better joint design is needed in the red

regions. Comparing this with step 5, the final design validation FEA result, the color scheme changes significantly. Notice the lack of high and low von Mises stresses on the FEA. This is because topology optimization removed volume from the areas that had a low effect on the part's structural integrity but corrected the sections where the part experienced high von Mises stress. This singular step is equivalent to repeating the FEA commonly up to 20 times from figure 1, since the optimization will be done by the computer in the click of a button instead of iteratively by a designer who runs the FEA this amount of times. Notice that a fundamental change in the flowchart is that having a sketch is optional since a preliminary shape is all that is needed by topology optimization to provide a functional part.

Instead of spending most of the time performing multiple FEA iterations, the designer now only focuses on appropriately inputting the constraints of the part, running the topology optimization software, and analyzing the final part. There are two main reasons for analyzing this final part, 1) to determine if the final optimized design requires shape optimization or 2) to determine if a redesign is needed.

Shape optimization "is to find optimal shape of a part or openings in a part" [19] and is not the same as topology optimization. This could be performed for various reasons and are also important in generative design part selection. The first is to ensure that no important parts are blocked off. For example, topology optimization may have formed difficult-to-manufacture sections for the part, even for a 3D printer. The designer can alter these sections and make the part no longer perfectly optimal but make it a lot easier to manufacture. It is also possible to shape optimize the part to make it even possible to manufacture with subtractive manufacturing. Some software allows input parameters like the smallest dimension size or manufacturing technique to help prevent the designer from performing a shape optimization step.

It is also possible that the constraints provided by the designer were not input correctly. Some of these constraints are not only the fixed sections or the forces, but could also be symmetry planes and manufacturing constraints in some software. Most of these can be noticed by closely inspecting the final parts for lack of symmetry or looking at the shape returned from the optimization.

Items	Case 1 11 CBS, 264 Design variables	Case 2 25 CBS, 600 Design variables
Iteration 10		
Iteration 20		
Iteration 40		
Iteration 100		
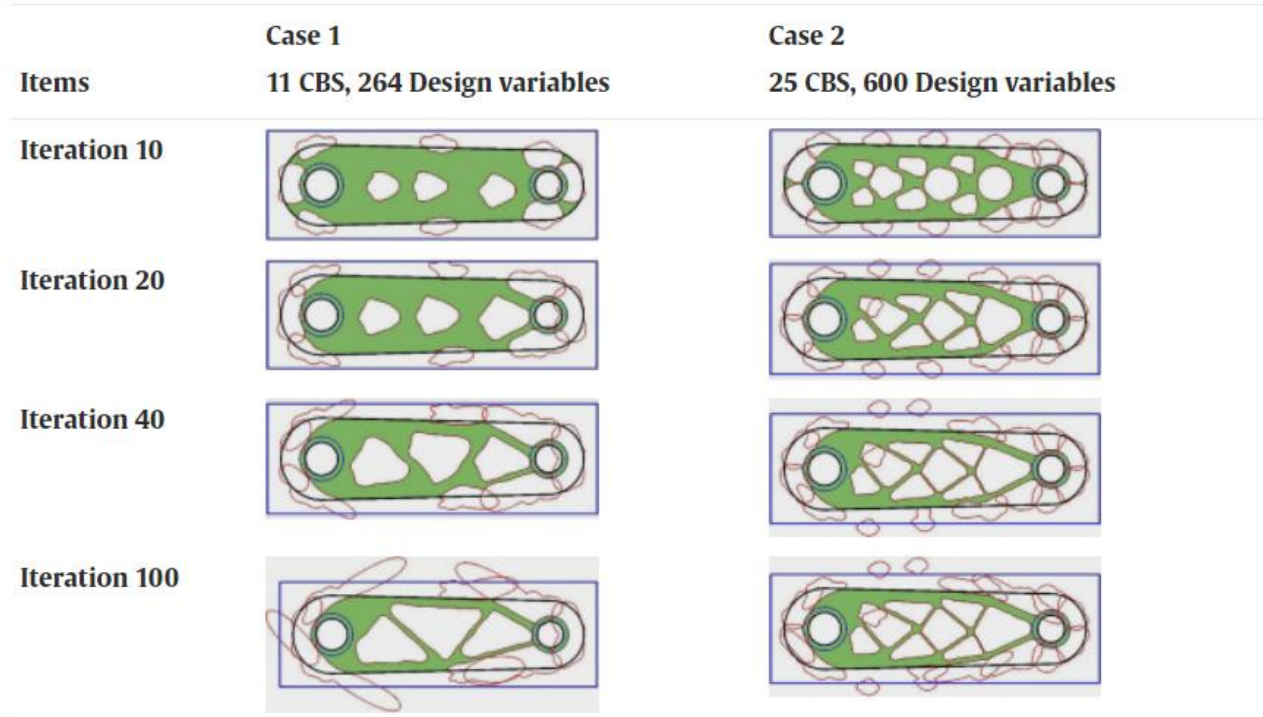
Figure 11: An example of a part optimized by topology optimization after 10, 20, 40, and 100 iterations. CBS referring to a closed B-spline shape and the amount in the shape, and design variables the amount of variables that can change. [20]

2.3 Generative Design

"Generative Design is a 3D CAD capability that uses AI to autonomously create optimal designs from a set of system design requirements" [21]. Generative design is commonly mistaken with topology optimization and even grouped, although they are not necessarily the same. Recall the statement: "The term 'Generative Design' has actually been around for many decades. The idea is straightforward, a parametric model that evaluates the outcome against some design goal and the automatically re-runs until the design goal(s) is achieved or optimized" [3]. This is not the same as topology optimization, which was defined as "…a mathematical method that optimises [sic] material layout within a given design space for a given set of loads, boundary conditions and constraints with the goal of maximising [sic] the performance of the system" [3]. A second source also emphasizes the difference between the two. Topology optimization is not new and has been around for at least 20 years. The source mentions that "topology optimization serves as the foundation for generative design" and that "generative designs takes it a step further by removing the need of an initial human-designed model" [22]. There are cases of large software companies, such as Autodesk, who offer generative design and topology optimization but decide to call everything generative design [3].

2.3.1 Generative Design Computation

Although not necessarily synonymous, much of the mathematical model of generative design can be seen in topology optimization due to the need to reduce volume and maintain the need for a von Mises stress below the yielding point of the material. The mathematical model for generative design will not be covered entirely in this thesis. However, a general explanation will be provided, and more is covered in detail by C. Dapogny *et al.* in 'Geometric constraints for shape and topology optimization in architectural design' [23]. Although the words topology

optimization and architecture are stated in the work's title, it is a helpful resource. Section 6.4 of this reference highlights a generative design example that will be referenced in a later section.

Generative design can be seen as the bottom-up process of topology optimization, which is a top-down process. The designer inputs the constraints and, if done correctly, will receive a plethora of parts (or the best of multiple solutions) from the software. The designer does not need to provide any preliminary parts or previous work.

In simple terms, generative design works much like a genetic algorithm. Genetic algorithms tend to mimic evolution in the outside world. In the case of generative design, parts are randomly generated in an initial population of specimens. Those that perform better are favored over those that do not perform as well and are kept for future populations.
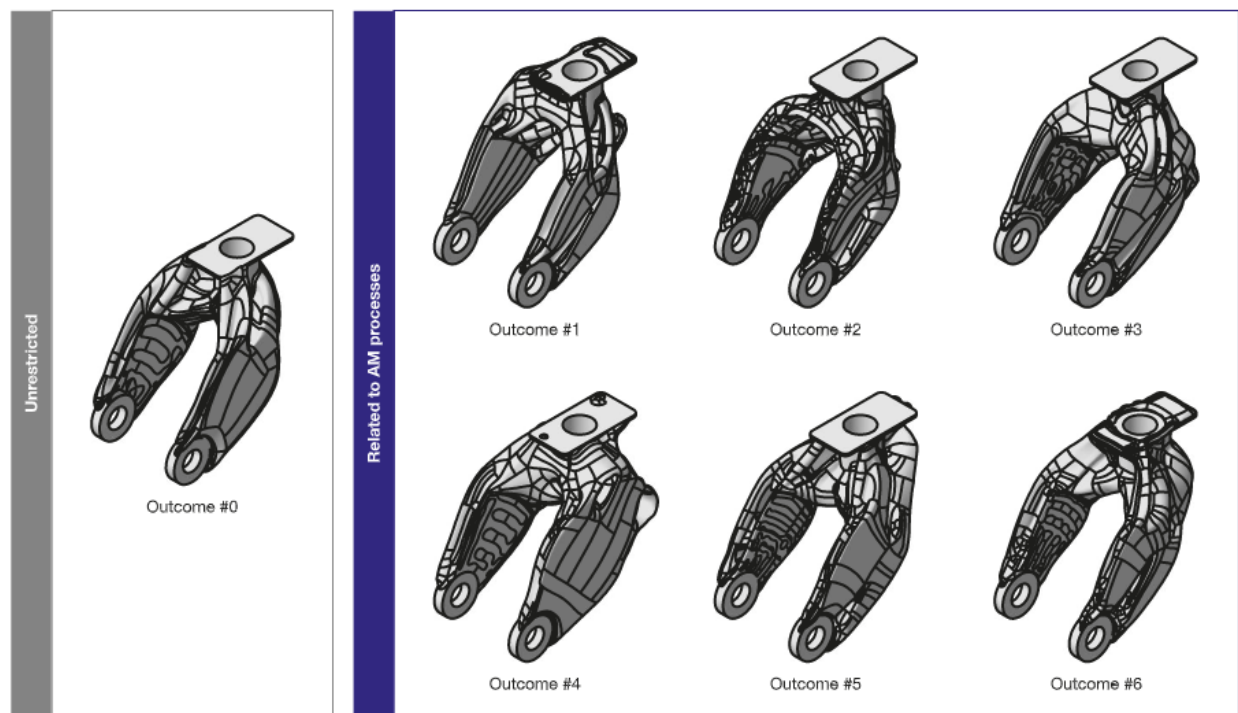
Figure 12: An example of different outcomes for the same simulation ran during a generative design study. One was unrestricted and the other six related to additive manufacturing (AM) processes. [24]

A random chance of mutation is also coded in, represented by changes in the location of the material in the parts. The algorithm is continued until the part converges to an optimized result [25]. Due to the randomness introduced by the software, the results can be different every time a simulation is run.

2.3.2 Generative Design Process

To run a generative design study, knowing how to set one up is essential. Usually, a generative design study has the constraints defined like a designer normally would in an FEA study. These loads, material choices, and fixed constraints are necessary for the study. However, more constraints must be defined for the study to run. The software usually describes these as starting, preserved, and excluded geometry. The preserved geometry is the volume that the generative design will not change (usually the point of connections to other parts of the assembly). The excluded geometries are the sections where generative design is not allowed to add volume. Lastly, the starting geometry is usually a reference for the generative design to work out of, but unlike topology optimization, it DOES NOT have to be included [24]. For an example of a configuration without a starting geometry, see figure 13. In this example, a design challenge from the Royal Institute of British Architects (RIBA) was studied. The example was utilized to structure my thesis investigation and will be explained in more detail.

The goal was to create electric pylons that could carry loads from electric cables with a minimum environmental impact. The design challenge provided a space in which the geometry should fit: a domain D of 15 x 15 x 45. The constraints of the analysis are the structure being fixed at the bottom support and having seven load points representing the electrical cables (see figure 15). Additionally, since the structure would be seen publicly, the designers decided to

27

"impose the symmetry of the structure with respect to the two planes containing the point (7.5,7.5,0) and parallel to the (xz)- and (yz)- planes respectively" [23]. A second example is section 6.4 of C. Dapogny *et al.* [23].
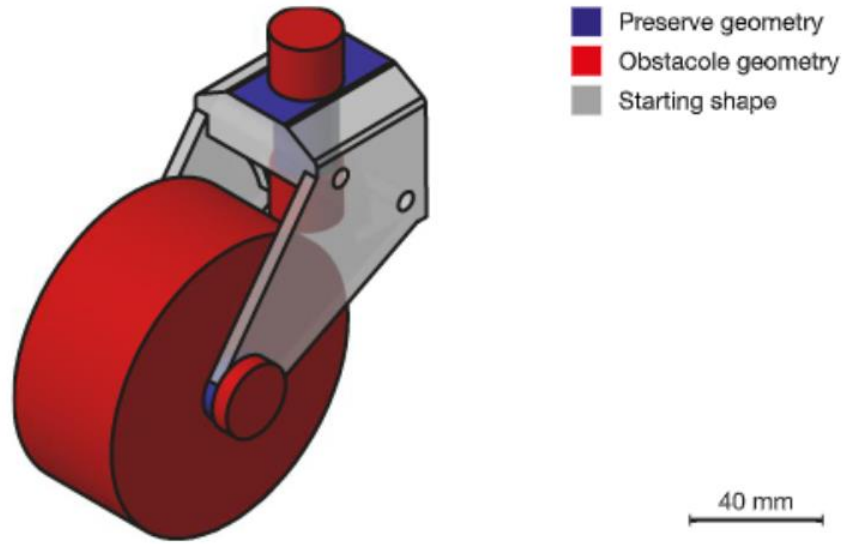

Figure 13: An example configuration of how to label the preserved, obstacle, and starting geometries. Note: a starting geometry was included "due to the complexity of the setup" [24].
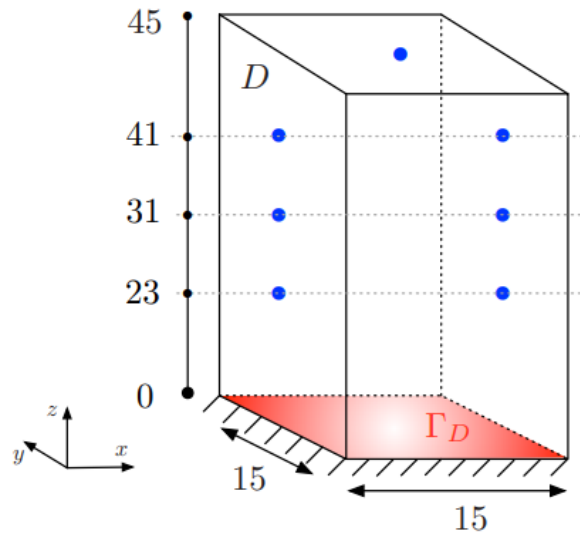
Figure 14: The boundary conditions for the electric pylon generative design study [23]

Notice in figure 14 that there is no initial geometry, unlike in figure 13. The designers included the locations of the loads/constraints and the design space. A total of six different load configurations were selected for the study (see figure 16), and multiple target volumes were chosen too. Figure 16 demonstrates some of the solutions acquired by the designers for target volumes of $V_T = 0.075|D|$ and $V_T = 0.05|D|$ where D was the 15 x 15 x 45 domain utilized.
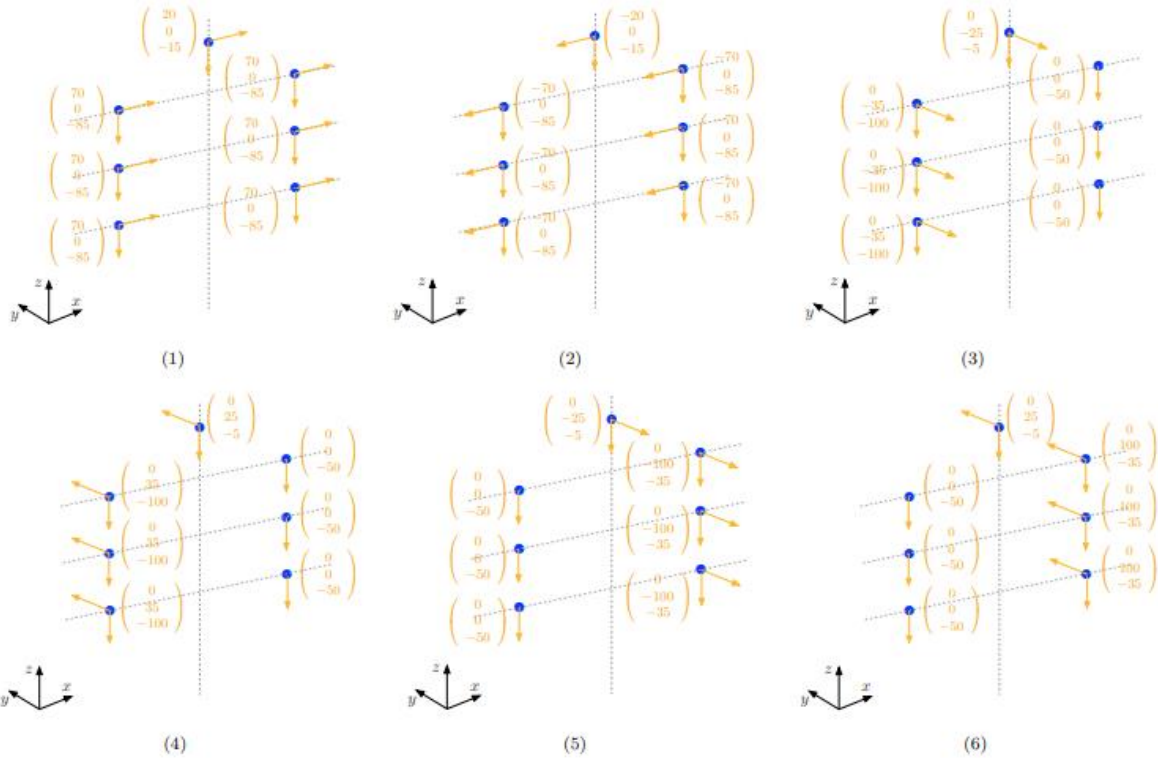
Figure 15: The six different load cases, in vector notation, explored in the RIBA study. Each blue dot is a location where a force is applied and the yellow arrows and vectors the forces [23].

It is seen in the study that the designers received various options, so many in fact that 6 figures are shown, all different possible solutions to the load cases provided and target volumes presented to the software. This would also be true in this research, but due to the lack of computational power, only one part is returned by Creo Parametric 9.0.0.0, the utilized software.
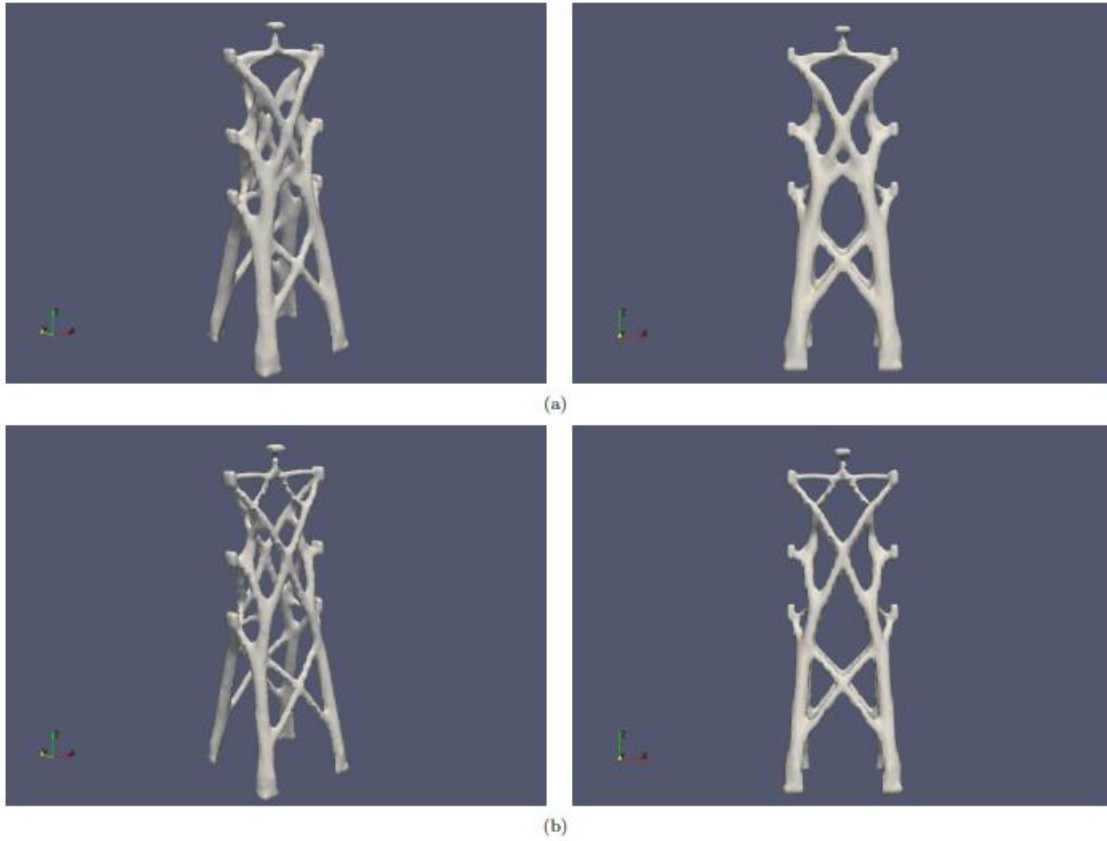
Figure 16: The results of the RIBA study for target volumes of (a) $V_T = 0.075|D|$ and (b) $V_T = 0.05|D|$ [23]

2.3.3 Designer in Generative Design

The designer's role in generative design is very similar to the role a designer plays in setting up a topology optimization study. The difference is that outcome selection is one of its most critical parts [24]. After every study, the designer must go through the choices and decide if a design is reasonable and manufacturable or a different design should be chosen. This can be done through inspection, computer-aided engineering (CAE), or utilizing a table to compare the different options. A table will usually present the models and weights assigned to different parameters, which change based on the field and specific application [24]. This will allow for sorting the outcomes, and the first or top few can be selected for further investigation. Sketching

is no longer considered part of the design process, although it could still be used as the designer desires in idea sharing or quick prototyping.
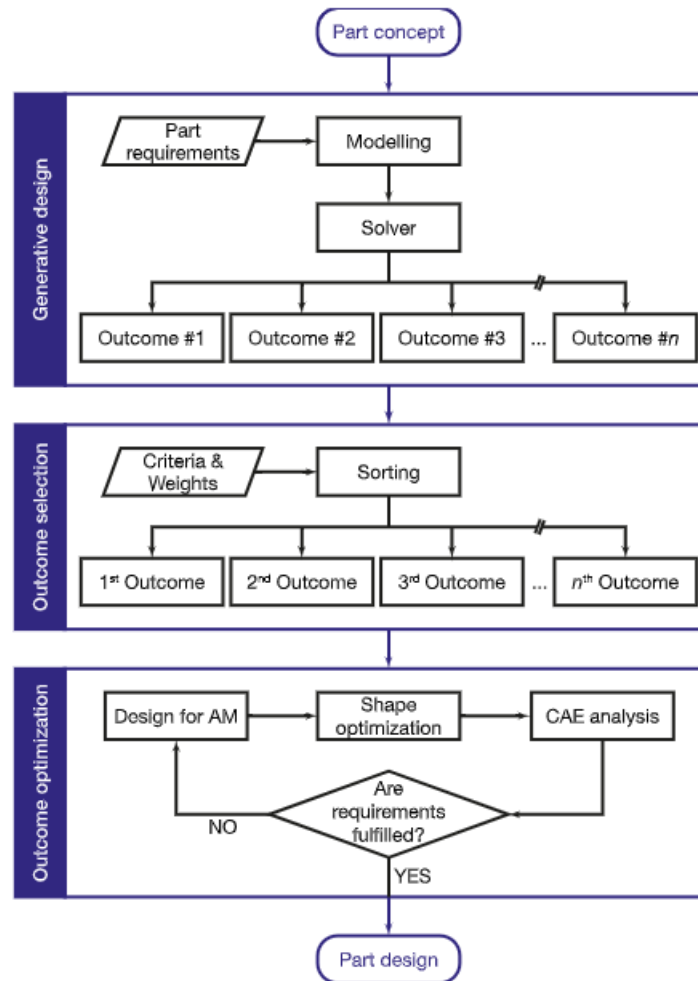
Figure 17: A generative design flowchart to design a part [24]

2.4 Bicycle Frames

Bicycles began around the 1800s, and since then, there has been an increase in the search for the most optimal design [26]. A lightweight frame with a high potential for acceleration and maneuverability is highly desirable when designing a frame. The frame must also resist heavy loading and sudden impacts and be stiff enough to maximize the power of pedaling into

acceleration [26]. Multiple studies have been performed on the different ways to optimize bike frames. Chung and Lee applied nonlinear programming to acquire the optimal dimensional parameters of a bike frame [27], Covill *et al.* found an optimal frame based on a regression model of 82 frames [28], and more recently, Decathlon released a bike "vision" created with generative design which as of November 2020 only exists as an artist's rendering [29].

2.4.1 Loads Experienced by Frames

According to L. Regenwetter *et al.* [26], bicycle frames experience three load cases. These three cases were explained in more detail by J. Vanwalleghem *et al.* [30] to be:

1. In-Plane Stiffness

The in-plane stiffness configuration is measured by fixing the frame at the head tube (the part that holds the handle bars) to prevent any in-plane motion. The first load (z-direction) is applied vertically at the bottom bracket or the rear dropouts. The in-plane deflection (x and z directions) is measured at those exact locations. Applying the loads at these locations allows for the assessment of the contribution of the front triangle to the total in-plane frame stiffness [30]. In-plane riding stiffness calculations can be considered as an everyday riding scenario. It is also possible that larger in-plane forces can be caused by uneven riding surfaces [26], such as pits, bumpy roads, or off-road riding.

2. Transverse Stiffness

Transverse stiffness measures the frame's resistance against transversal loading. The rear axis is held in place to prevent transversal motion, while deflection is measured in the bottom bracket [30]. Though transverse loading is relatively small during normal cycling, deflection can still be significant and contribute to reduced power efficiency [26].

3. Eccentric Stiffness

Eccentric Stiffness configuration attempts to mimic the pedal force. This load is purposely applied off-center, so there is a torque and a force at the bottom bracket. This results in a rotational and vertical displacement [30]. Eccentric stiffness is meant to capture an acceleration from a stationary scenario where the rider applies their whole body weight to a single pedal. If the rider decides to pull on the handlebars, even more force is applied [26].

2.4.2 Generative Design Frames

The current design process of creating bicycle frames with generative design is a considerable challenge. Not only do the bikes have to hold these loads, but they also fatigue and wear. The bone-like geometry from generative design is not only questionable in terms of the structure's shape but also seems to be out of the picture for racing bikes due to the "aerodynamic mess it can be" and the lack of formations of streamlines [29]. Commercial users do not need these high-performing bicycles, and reducing the frame's volume can also benefit mobility. An optimal design with less volume would also require less material, and 3D-printed metal parts will be more environmentally friendly. As of right now, Decathlon has a generative design created fork that is only on a concept bicycle (see figure 18)

As we approach the thesis investigation, one of the questions to keep in mind is if generative design sacrifices the frame's structural integrity. In 2000 the *Union Cycliste Internationale* introduced a regulation that specified that bikes in UCI competitions must weigh a minimum of 6.8kg to prevent companies from compromising the structural integrity of bikes [29]. It is tough to consider the many loads experienced, and optimizing a design is a lot harder than optimizing a design on a single criterion. Generative design can consider the loads in a direction specified by the program, but fatigue and constant loading can change the material properties.

Figure 18: Decathlon's concept bike frame created with generative design in the majority of the front section [31]

Although there are generative design studies that could consider fatigue (and even some that can simulate thermal properties), only static loads are considered for this work. This is because the

goal is to determine how well generative design models hold the loads they were designed to hold.

Chapter 3: Methodology

3.1 The Investigation Overview

In this investigation, generative design was used to create small-scale models of possible frames and were compared to a small-scale model of a standard bicycle frame. The frames were tested on an Instron machine to determine if the models presented by generative design were accurate and better than the average frame. Creo Parametric 9.0.0.0 was the software used to run the generative design studies.

To compare the frames tested, mass and load carried will be considered. Price could also be considered in a real-case scenario. However, the price differences would depend on the volume used since it is the price of the material printed. The prototypes were made to experimentally test the values obtained in the simulation and compare them to a benchmark bike frame.

3.2 Creo Parametric

Creo is one of the software that has generative design capabilities. As described earlier in the background section, multiple constraints must be considered to set up the generative design study. These basic constraints are fixed points, locations experiencing loads, selected symmetries, and material properties. This is perhaps the easier part of setting up the study since simply importing a shape into Creo Parametric does not guarantee a successful output part by the generative design analysis. A basic bicycle frame was imported from GrabCAD [32] to start the study. The model is for a bicycle frame with 26" wheels, and the user who uploaded it claims to have used a Ribble sportive racing frame geometry as the dimension. The dimensions were measured in Creo Parametric to confirm that the model dimensions matched the specifications and could be used in the thesis.

3.2.1 Setting up the Model

To prepare for the 3D printing procedure, the model had to be scaled first to account for the printing bed sizes available to me. There are 3D printers capable of making actual-sized frames out of plastic or even metal, but none are openly available for me to perform a study on a frame printed in one of those. Upon measuring the longest dimension of the frame, it had to be scaled by a factor of 1/5 to fit in one of the 3D printer beds. With this accomplished, the model can be modified to prepare for generative design. Whether performing generative design study or a topology optimization study, every point of connection that needs to be preserved must be

sketched on top of the existing CAD model and extruded through the model. This step may not seem odd once the generative design study is run, but it will remain a strange step in a topology optimization study. This will create two overlapping models, and it may seem like they are interfering with each other, but they are not, and this will be necessary. The key part to this step is selecting the "extrude" button for each sketch, and in the extrude "Body Options" click on the "Create New Body" check box. Selecting this box ensures that the new overlapping body does not simply add itself to the existing model with an addition Boolean operation automatically. In the "options" tab, the depth can be selected to go up to a reference so the new body is as close as possible to the previous frame segment.
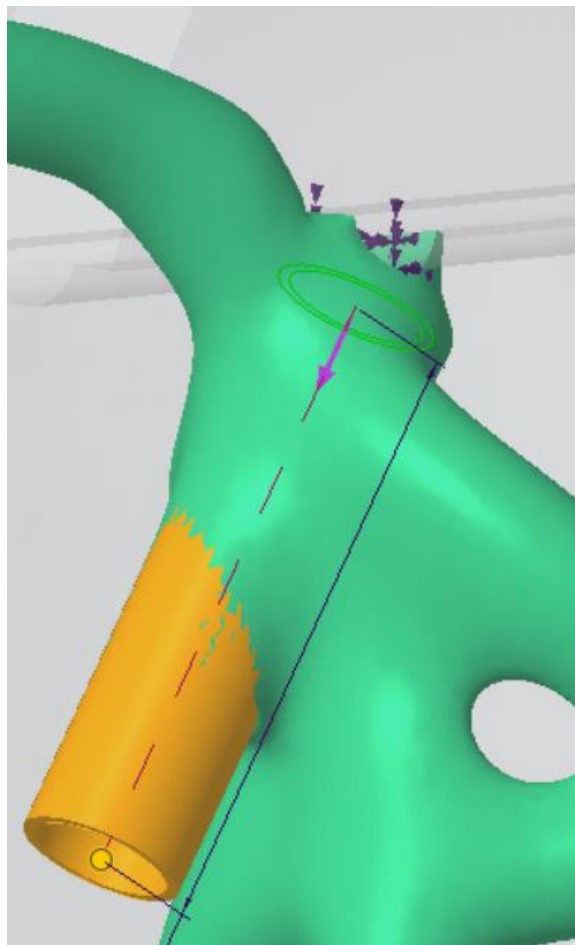
Figure 19: Visualization of what an extrusion through an already existing part looks like. The clipping through the part is normal and this is needed to proceed with the study.
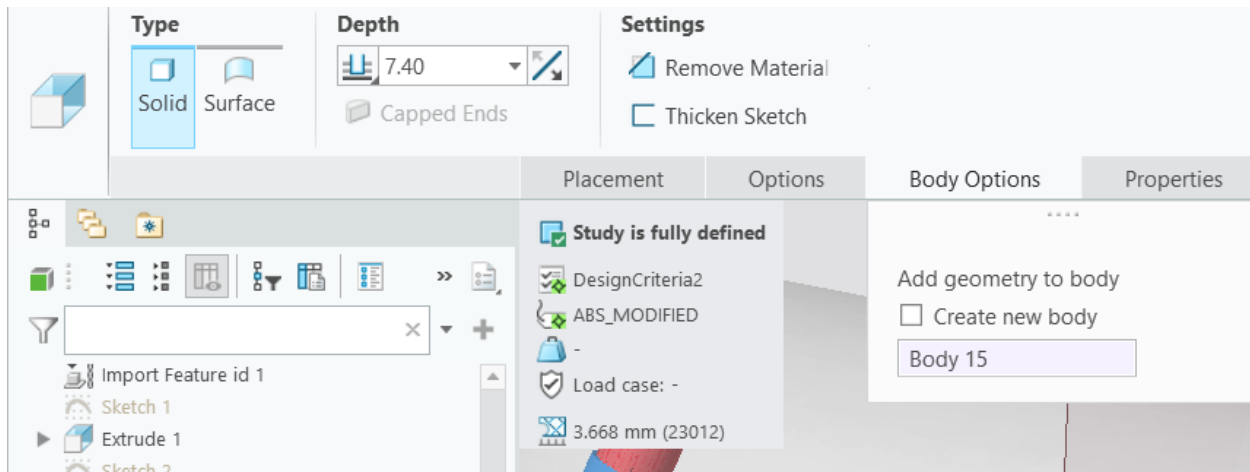
Figure 20: Pictured on the bottom right of the image, the "Create new body" checkbox

In the bicycle frame specifically, I had to do this five times. The first is the segment making contact with the bike's fork, which holds the front wheel and handlebars. The second is at the bottom of the bike, which holds the crankarm where one pedals. The third location is the part of the frame that holds the seat post, where the person's weight is held. The last two are symmetric, the connectors holding the back wheel (dropout joints). Two are needed for the back because the frame directly holds the wheel and the front part is the head tube, which just holds the fork of the bike. The first three were simple to recreate since they were hollow cylinders. I chose a flat part of the cylinder as the sketching plane and drew two circles on that sketch plane. These two circles were the whole sketch and were extruded up to the face on the other side of the cylinder. The dropout joints had a much more complex structure. These were composed of line segments and a combination of arcs traced after determining their center's location. One was extruded, and a symmetry plane had to be added. This plane is essential because it will later be used to define the coordinate system for the direction of the forces and as a symmetry constraint in the study. For now, it was said to be parallel to one of the back wheel holders. The distance was measured between these back dropout joints, and the plane was said to be offset by half that

distance so it would perfectly go through the bike frame in the middle. I used the "mirror" command to mirror the previously created body to the other side.

It is also important to consider if the 3D printed model can be tested and how it will be set up on the Instron 6800 Model Series (Mid-Range testing system). As a precaution to give more options for testing, I decided to sweep from the front bar a solid cylinder. This cylinder would provide a point of contact for holding the part during the experimental tests. The cylinder came out of the fork straight down to have a minimal chance of failure during the experimental section and was excluded from the generative design study. After the results, the body could be made visible again. I added a second point of contact where the seat is so the Instron machine can push down at that point.

Even more bodies must be considered when setting up the study, specifically the excluded geometries. The main one is the back wheel, which must be included in the model so the provided frame does not interfere with any possible wheel position. As mentioned previously, the bike frame was modeled for 26" wheels. Utilizing a resource [33], I modeled a thin cylinder with the approximate dimensions of the 26" wheels in the symmetry plane. This circle was extruded equally in both directions of the plane for it to stay centered.
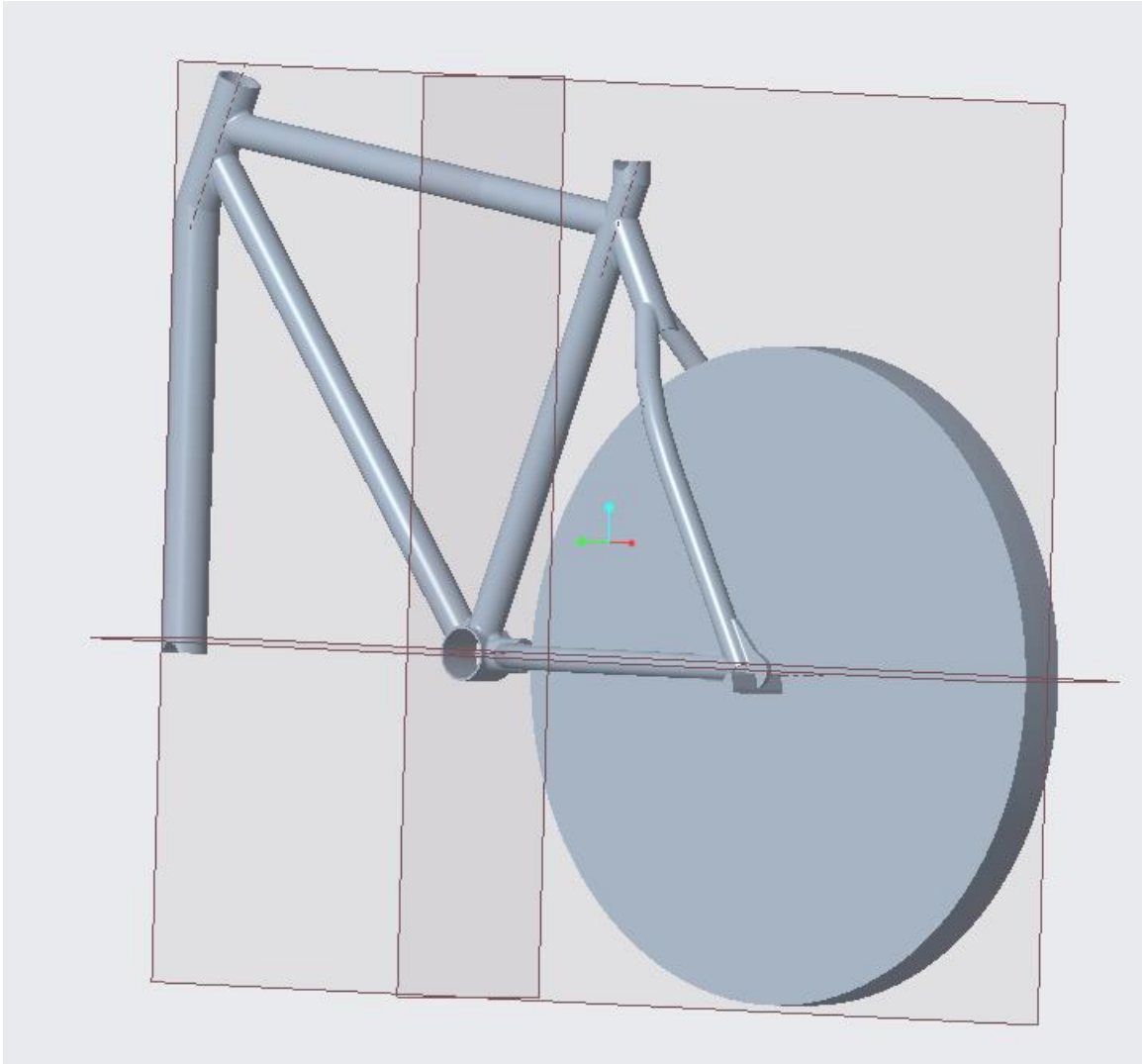
Figure 21: The modified original bike frame, including the back wheel and contact points

Also, note that bikes usually have the back wheel holder open on the bottom for the back wheels to go in. This must also not be obstructed, so an additional body was created to prevent this from happening. The front cylinder segment where the bike fork goes could not be obstructed, so a cylinder body was also modeled there. This is the same for the pedal location since it must remain an open hole for the pedals to be inserted in. The contact location added on

the seat could also be obstructed in the process, so a future excluded body was added there to maintain the shape.
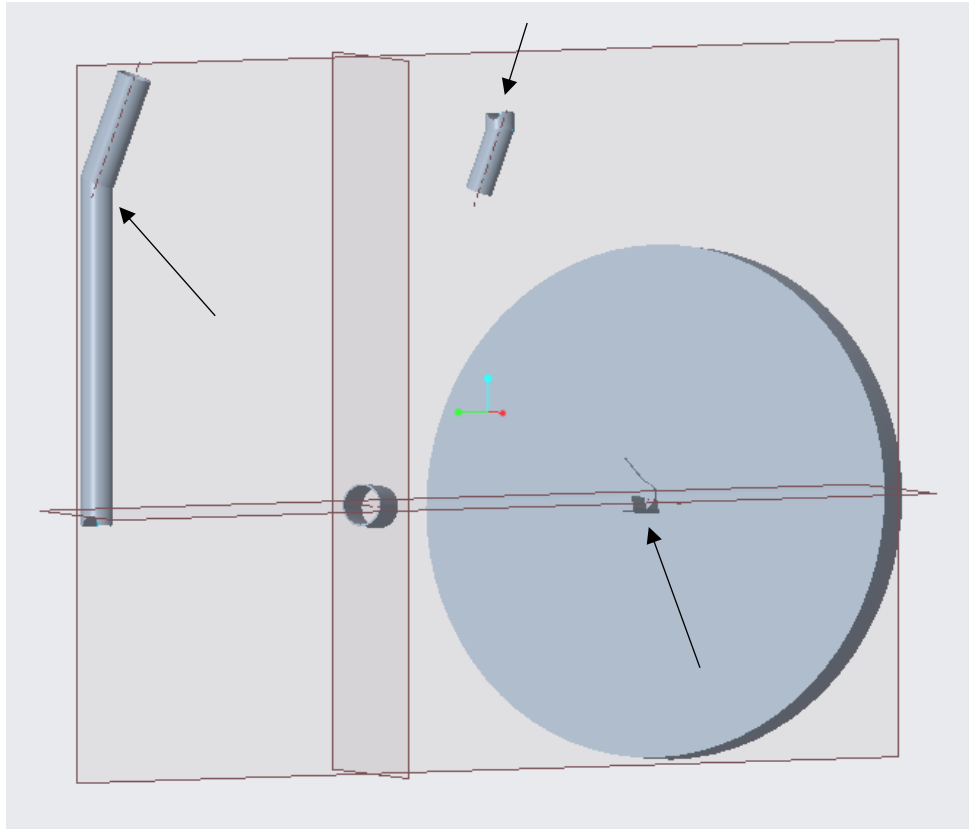
Figure 22: The three contact points (denoted with arrows) and the study's obvious preserved/excluded geometries.

Currently, one plane in the study goes through the bike frame, and I had to add two other planes to be able to select a set of orthogonal directions for the direction of the forces. Any three orthogonal planes would do since they would allow for three basis vectors to be created from them and span the design space. However, I decided to try and create a traditional X, Y, and Z axis plane since the force investigated will be going in the upward direction. This will simplify the process when running the generative design study. Three orthogonal planes were created using points and other references on the frame.

The last part of the setup for a generative design model is to remove the imported reference bike frame. If this bike frame is kept as a "starting geometry," then the study becomes a topology optimization study. In the software, I would select the imported bike frame as the reference geometry (which would gray out) during the simulation setup. Then the bodies that seemed to overlap with the frame would be selected as the preserved geometries.
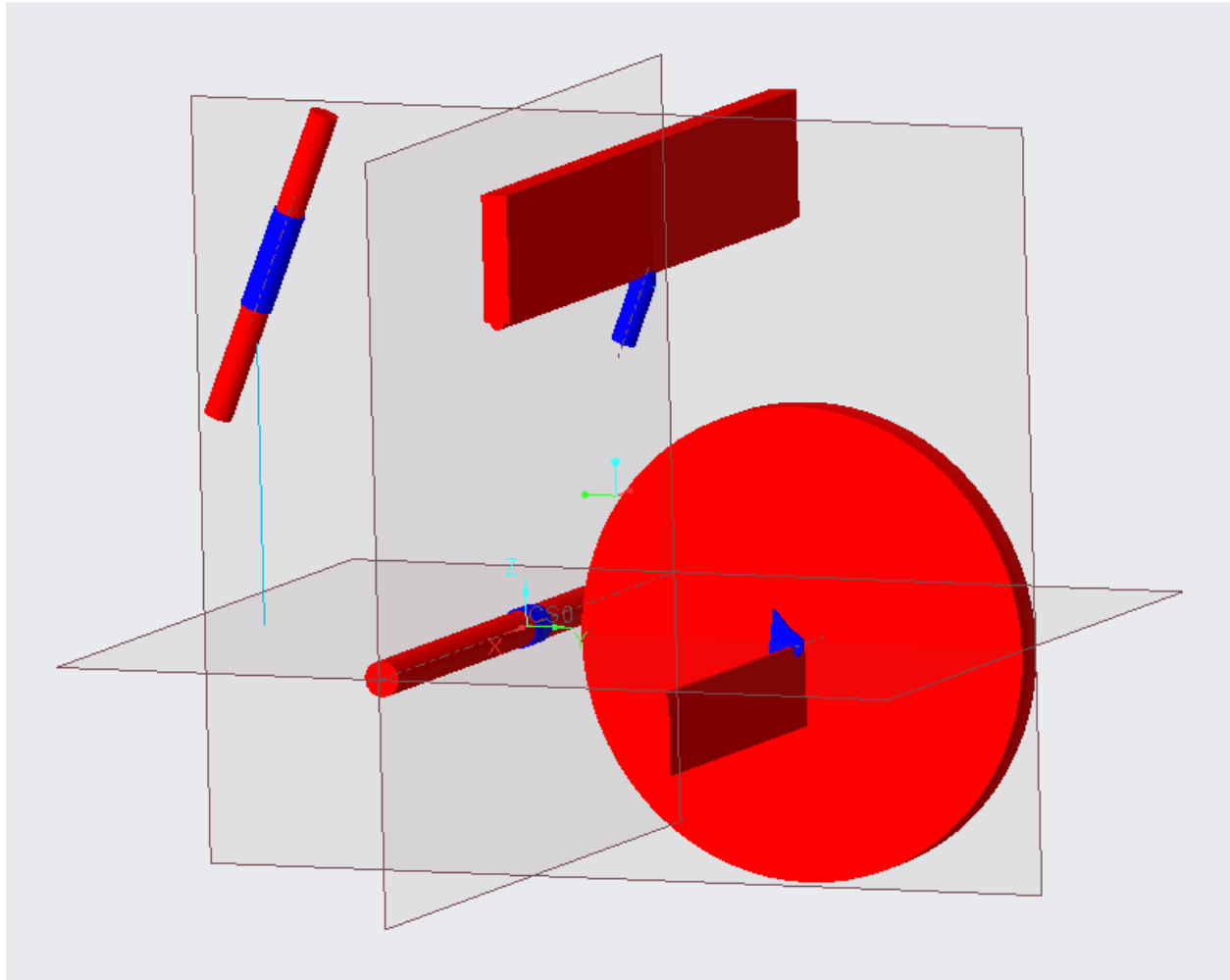
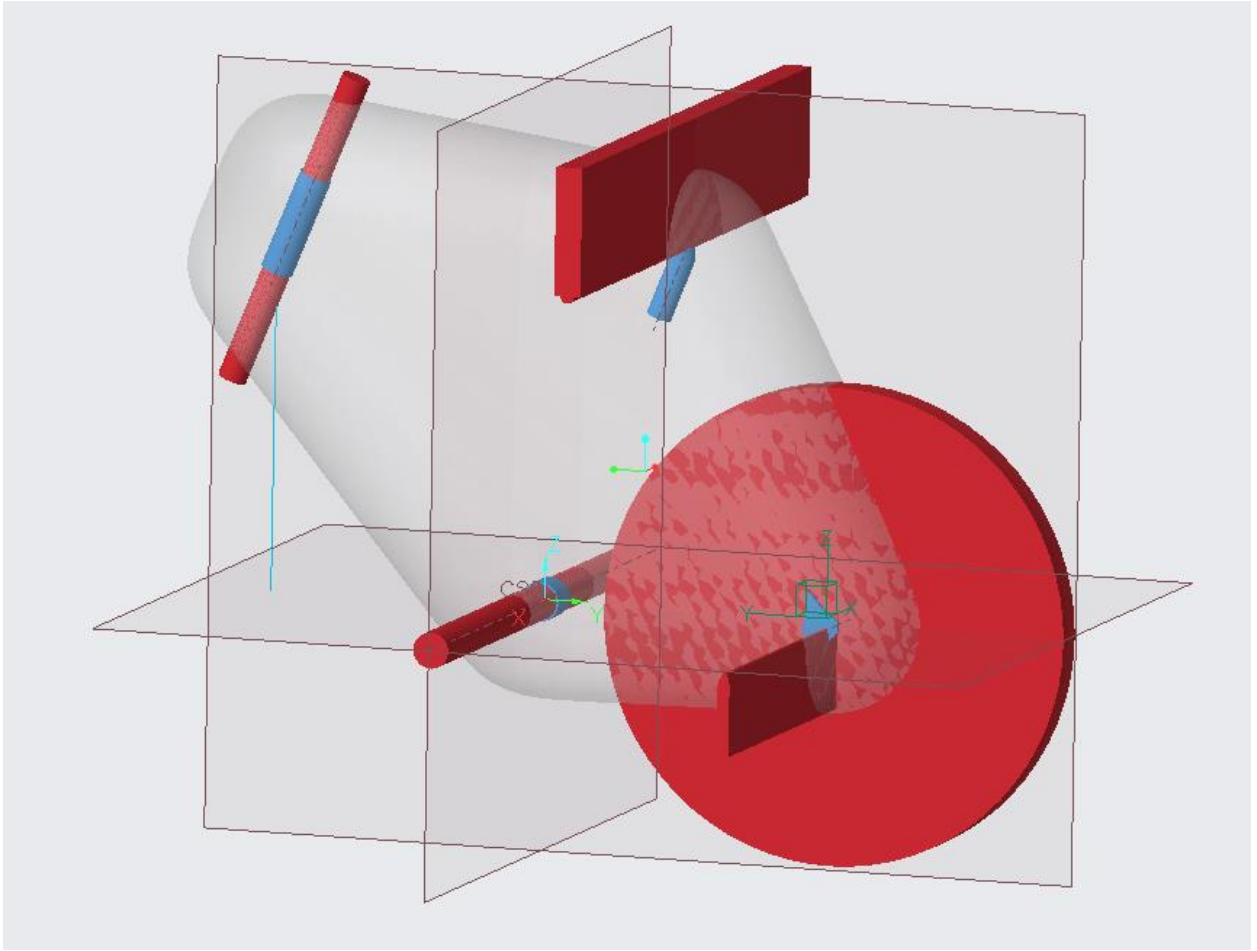**Figure 23:** Preserved (Blue) and excluded (Red) geometries used in the generative design simulation

In my case, a generative design study, I deleted the frame by utilizing an "intersection" Boolean operation. I was left with four bodies that seemed to be floating in the air. This Boolean

operation keeps the intersecting parts, so selecting the frame and any new body I added within the frame was sufficient. These floating bodies are the wanted result, and now the generative design study can be started.

3.2.2 Running the Generative Design Simulation

After setting up the model, I went to the "Applications" tab at the top of Creo Parametric to select the generative design simulation. After clicking this, a control menu window opens with the options to select the starting geometries, excluded geometries, and preserved geometries. The correct geometries were selected; recall that a starting geometry does not need to be selected, and the starting geometry will form automatically around the preserved geometries.

When selecting the constraints and loads for the study, I had to consider what could be studied in the Instron, making sure that the simulation was as similar to the real measurements as possible. I decided to measure In-Plane Stiffness, and in this case, it would eventually be found to be most effective by making the pedals and seat fixed with the forces acting on the locations of the front and back axles. The forces on the back axle would be varied until a mass related to the current bike frame model is found, or an equivalent of the mass held by the current bike frame is used. To complete the study setup, "Add Design Criteria" has to be selected and configured.

Figure 24: The recommended starting geometry (Transparent gray) based on the included (Blue) and excluded (Red) geometries provided
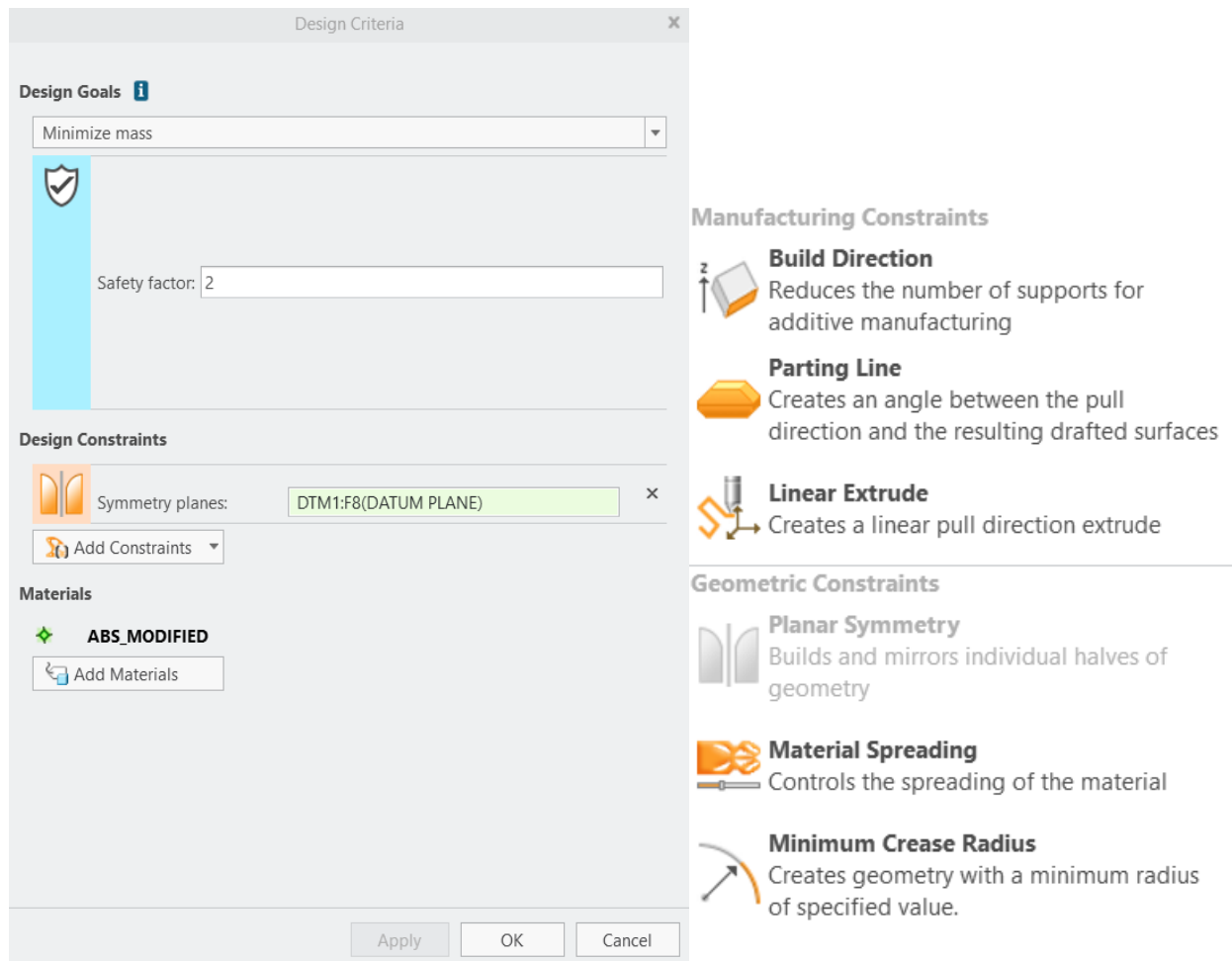
Figures 25 - 26: Figure 25 (Left) shows the Design Criteria options where the goal, constraints, and materials are selected. Figure 26 (Right) shows the possible options which can be selected under the design constraints. Only Planar Symmetry was selected in this study.

Upon selecting this option, a new window opens with the options to maximize stiffness or reduce mass (both described in section 2.2.1). I minimized mass, attempting to keep a safety factor of 2. This is important because a bicycle frame snapping while a rider is on it would be a huge problem, so ensuring the frame's In-Plane stiffness is safe was part of the consideration. Design constraints are also added on this tab. I only added the "planar symmetry" geometric constraint. After looking at some of the initial models, I did not deem it necessary to add the manufacturing constraints since the models already looked manufacturable. The default ABS

material was selected for the parts, slightly modified according to the Stratasys ABS-M30

datasheet [34]. The last significant step is to specify the Failure Criterion in the

Figure 27: The material properties for the ABS utilized. Note that the failure criterion must be specified

material definition, which was my modification. In this case, the failure criterion was specified as the distortion energy (von Mises), and the Tensile yield strength was required for the calculations to work. The ABS-M30 data sheet specified this [34]. A small modification was performed before printing. I added a rectangle that would connect the back frame bars together (these would usually be held together by the back wheels). The results of the generative design studies can be found in the results section. The symmetry may be changed from isotropic to orthotropic but the material properties in the X, Y, and Z directions must be known; Specifically Young's modulus, Shear modulus. Poisson's Ratio, and Coefficient of Thermal Expansion in all 3 directions. By printing the material in the plane of the Instron test, I assumed there would be a good approximation of the isotropic properties.

3.3 3D Printing

A 3D printing process had to be performed to test the parts, and a printer had to be selected from the available options. The printer had to be reliable, and there should be minimal common 3D printing defects. Some available printers to select from were a Prusa MK4, Markforged Onyx Pro, Stratasys F120, or a Creality 3D resin printer. The main two printers being considered were the Stratasys F120 and the Creality 3D resin printer. The resin printer was being considered because it would provide for an isotropic part since it would print using resin that hardens with light. However, this resin is not as well documented as the material properties of the Stratasys ABS-M30. The printer also usually has low availability and a smaller print bed than the Stratasys. For these reasons, I decided to use the Stratasys and print the parts in an orientation that would have the most negligible effect on the Test due to the anisotropy.

3.3.1 Printer Settings

The Stratasys printer uses ABS-M30 filament as the printing material and SR-30 as the support material. SR-30 is very important in this process because this support is soluble, so any supports which could provide extra strength to the part are dissolved. To set up the print, the generative design models were reconstructed in Creo, selecting the "Generate Design" button available on the top right after the conclusion of a generative study. The model was saved as a standard triangle language file and opened on GrabCAD, the printing software utilized on the Stratasys printer. All settings were kept regular except the infill density, which was turned up to 100% to replicate the generative design models as accurately as possible. The model was printed in the orientation so the part would be flat on the side. Each print took approximately four hours to complete.

3.3.2 Printed Parts

After the prints were complete, I simply scraped each printed part off the printer's bed. Using a flathead screwdriver, clipping pliers, and needle nose pliers, as much of the visible support material was removed by hand. To remove any leftover support material, the parts were left in a circulation tank composed of water and Ecoworks cleaning agent tablets made explicitly for dissolving the SR-30 support material. After removing the parts from the bath and rinsing them with water, they were ready for testing (see figure 28).
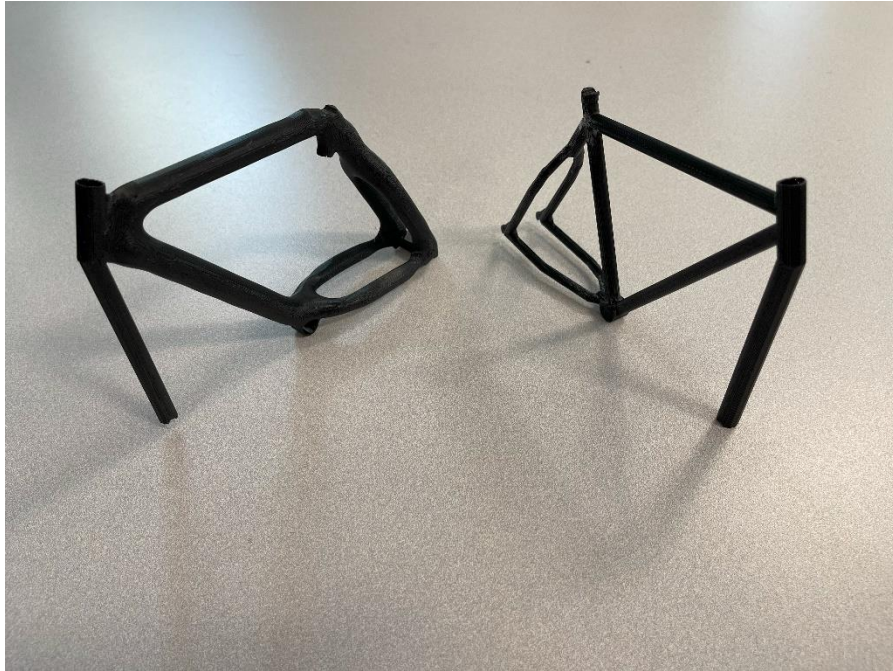
Figure 28: Two of the 3D printed models using the Stratasys printer
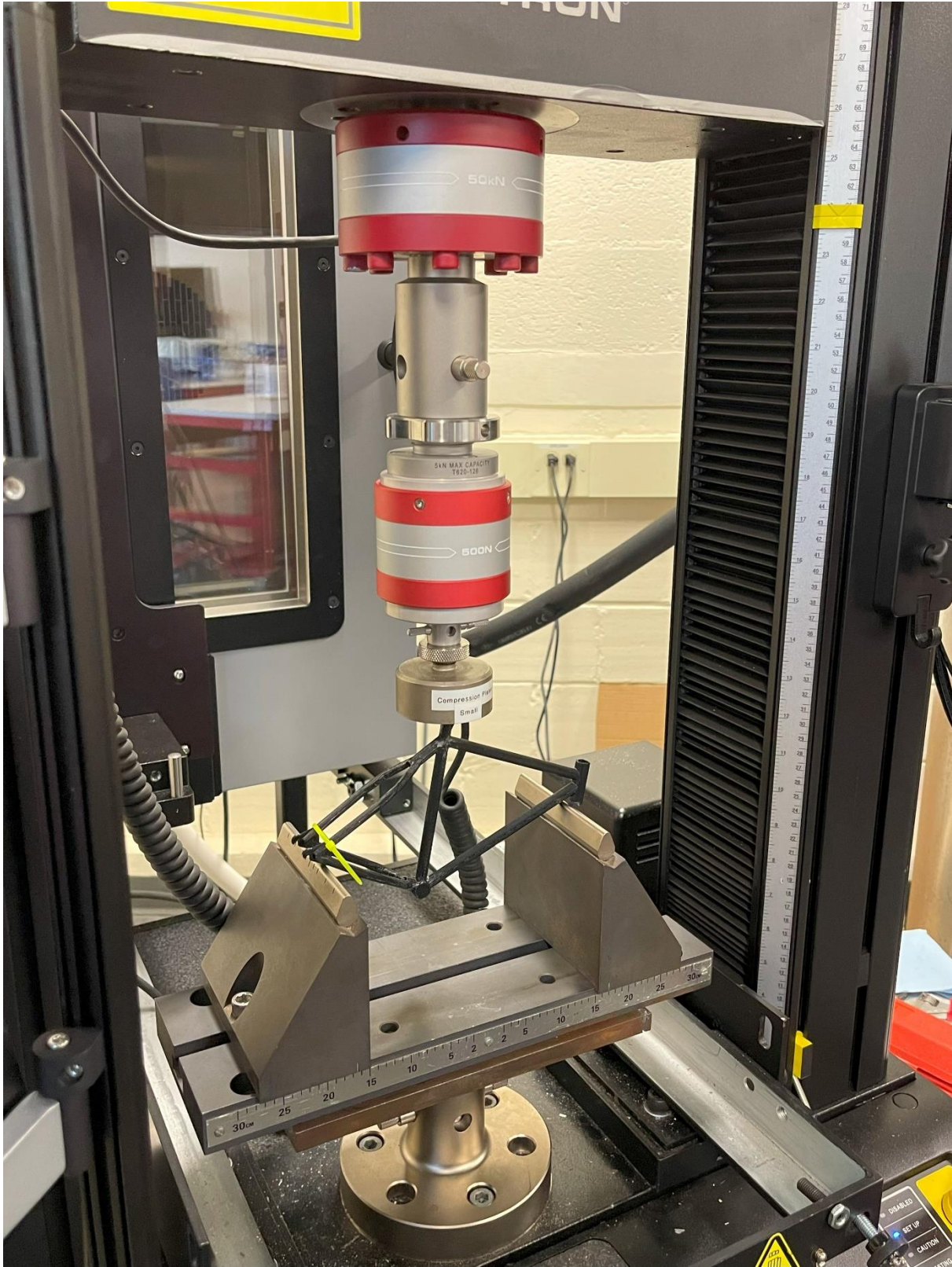
3.4 Instron

I had to create a testing program on an Instron 6800 Model Series (Mid-Range testing system) to test the parts. The Instron utilized has a force capacity of up to 50kN, but this range was unnecessary when testing these parts. Instron machines are usually used for a set of standard tests, so running this study required creating a new process for it.

3.4.1 Instron Setup

First, I had to set up the Instron's mechanical configuration for the study. The frame had to be held at two points, so the bottom fixture for the 3-point bend test was used (a force diagram can be found in figure 45). This is to attempt to replicate the normal forces experienced by the frame from the front and back wheels as accurately as possible. A small compression plate was used to apply the force instead of the usual bend fixture that is used for the 3-point bend test. The

compression plate allowed for slipping when necessary, and since the contact point was small, this load is still approximate to the point load on the simulated models. For the original scaled-down bike frame, a zip tie had to be used to restrict the motion of the back of the frame. This would usually be held together with the back wheel.

The default load cell used in the machine is a 50kN one which is less accurate than other load cells that are used to measure less force. To collect data for the original bike frame, I inserted a 500N load cell. The bike frames were centered using small marks on the side of the bottom fixture. It is very important that the frames are centered because any imperfection in the placement could lead to the frame bending in unwanted ways and possibly even flying off the machine. The stopper, a yellow slider on the side of the machine, was set in case the machine did not stop. With the physical setup ready, I had to set up the software and input the parameters for the new study.

Figure 29: Testing the original frame in the Instron machine
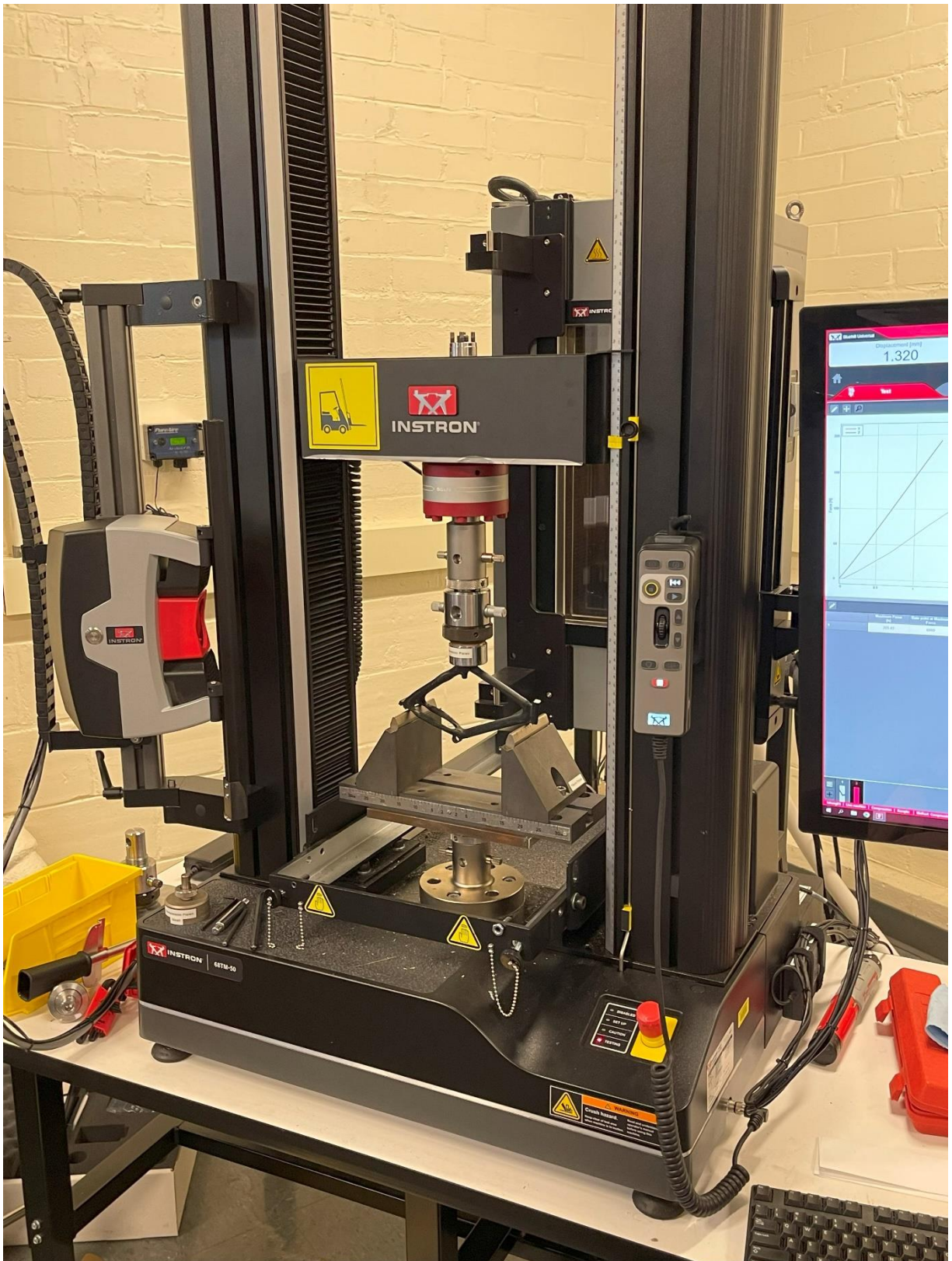
**Figure 30:** Testing a 200N-generated model on the Instron machine
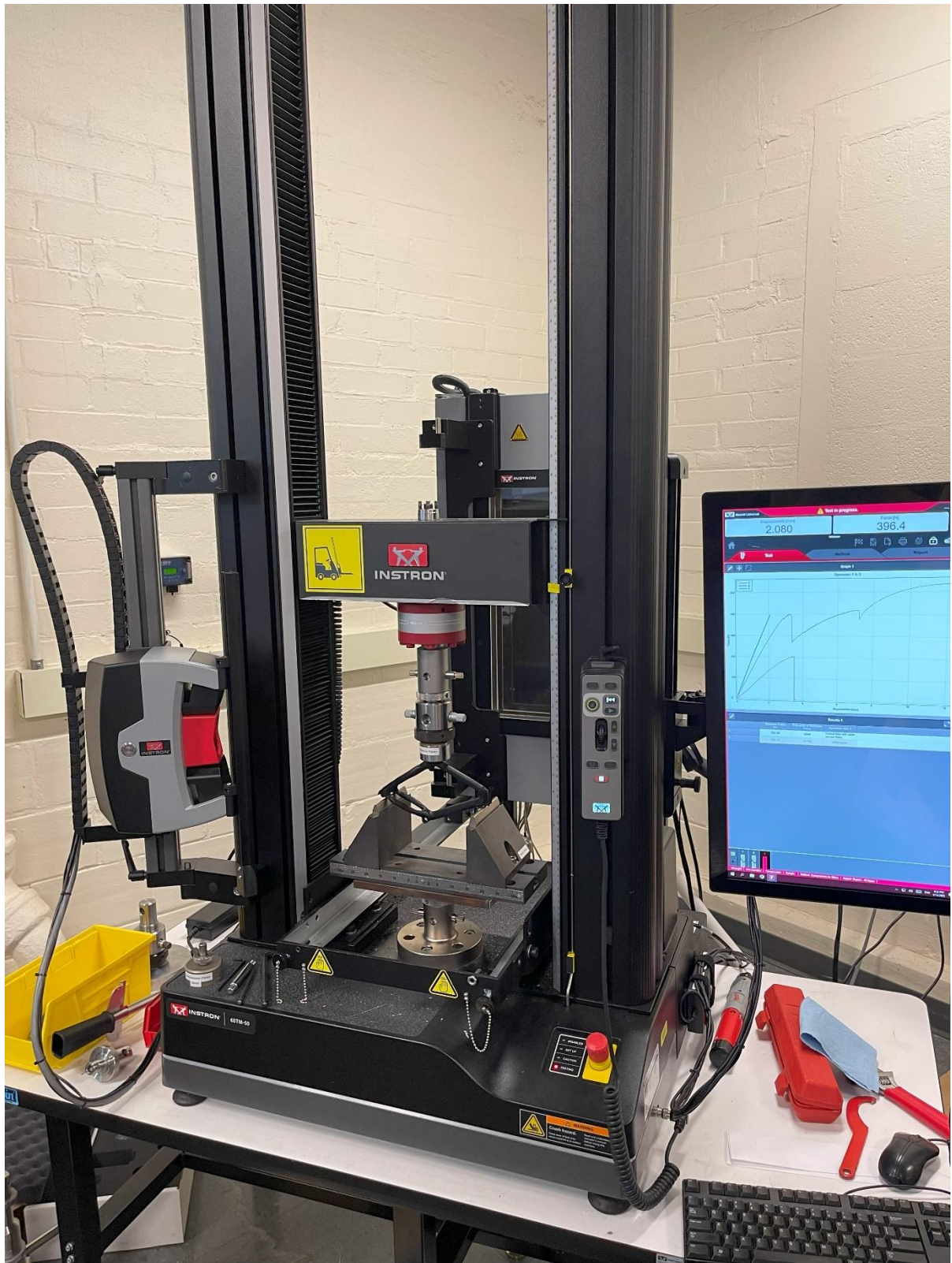
Figure 31: Testing a 250N-generated model on the Instron machine

3.4.2 Running the Instron testing

I ran a compression study that would record displacement and force. The main parameters were selecting what would be displayed on the machine report, the measured parameters, and the test parameters. I set the rate at which the compression happened at 1.5mm/min to make sure the compression would be slow. The frame being tested was placed in position, and the machine was calibrated using a large "calibrate" button visible in the screen prompt. The load cell was lowered every time as close as possible to the contact point using first the arrows for extensive movements and the scroll wheel for more minor corrections. The study was run using the play arrow on the same controller and stopped with the red square button on the bottom of it. The data is automatically collected by the Instron. The only steps that I had to take in between tests were switching the sample, naming the sample, and lowering the load cell. The bottom fixture of the 3-point bend was all that was used to hold the models in place. No tape or any adhesive was necessary.

After I completed all the tests, the data was exported from the Instron as a CSV file, and the report was generated in the form of a PDF. This CSV file was configured to contain the values for the Force-Displacement graph.
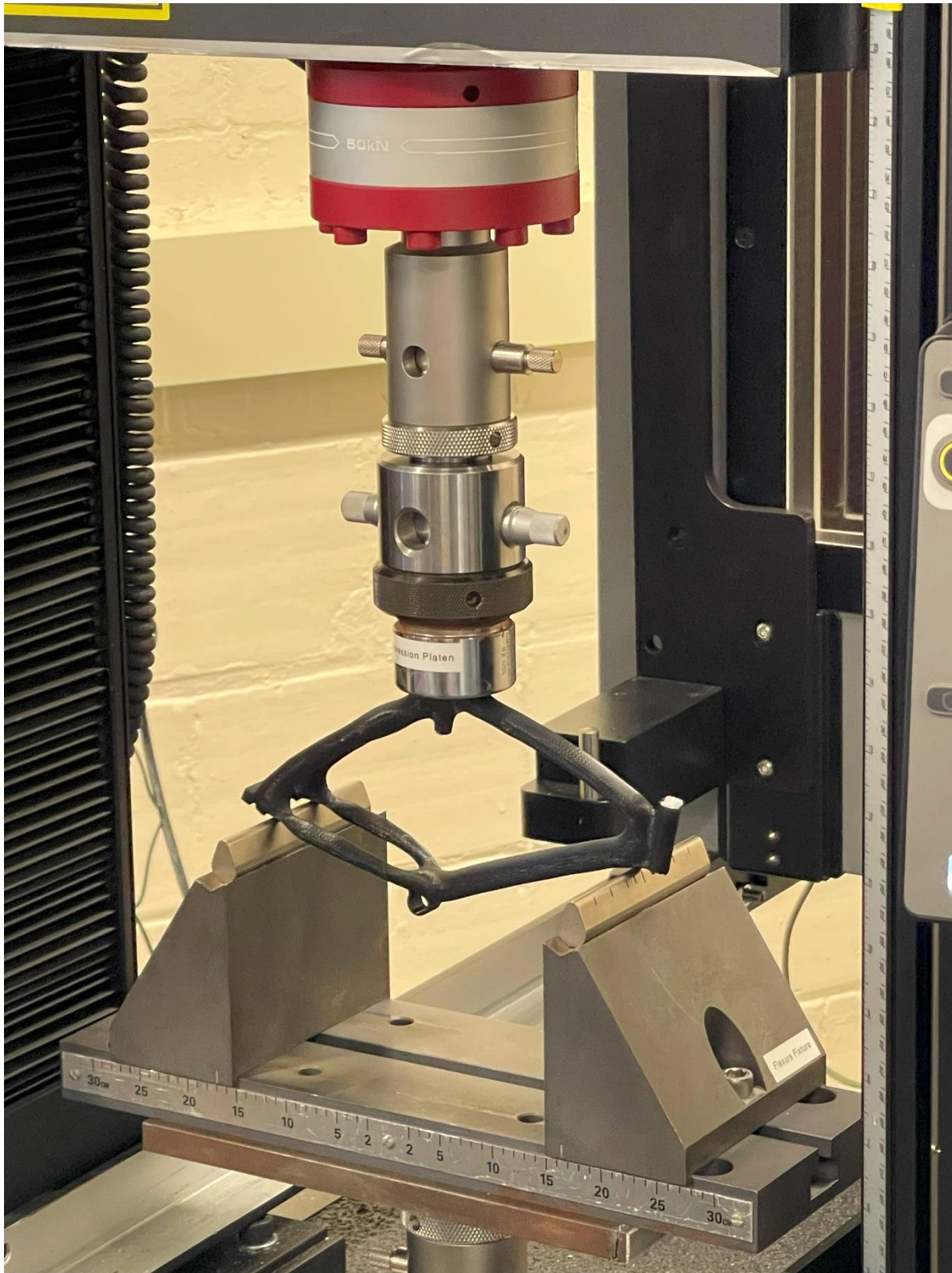
Figure 32: The 250N generated model with visible strain (white) and deflection

Chapter 4: Results

4.1 Generative Design Models and Challenges

To acquire the results from the generative design program, many changes had to be made to the force and fixture constraints. Ideally, the computed model would have been acquired with the same load cases as it would be tested, but there were some things that were discovered through the generative design process. The first method was adding fixed constraints at the two wheel axle locations and the force application downwards on the seat location, however this method was an incomplete definition of the problem. This did produce converged results, but they were not necessarily applicable to a bike frame since the lack of a force or constraint on the pedal location caused the solution to look like an arc and completely ignore the pedal location on the frame. This was reasonable by the part of the software since if that part is experiencing no force; it is reasonable to assume nothing has to be connected to it. Additionally, there was no option found that forced the generative design model to connect these points even if there is no force on one of them. This and other convergence failures are shown in the following figures, attempted with different configurations. In fact, one of the best configurations for the study initially failed before starting to converge. It is important to note that, although on the top left of the figures, the software states "Optimization Finished," it is not necessarily an optimization that an engineer would use because of the warning symbol next to it. This warning symbol occurs because "the optimization did not converge within the maximum number of iterations." These iteration values can be changed in the "study settings" option. However, the computational power changes and the current model optimizations already took 100% of the CPU, so they were

kept at the default Creo values. Note that running these studies is not cheap in terms of

computational power; At times, some of the studies took approximately 40 minutes, and the

computer used was an MSI GS66 Stealth with an i7-10750H processor. Some models did

converge, but the points were not necessarily connected, so the model had to be discarded as a

viable option.
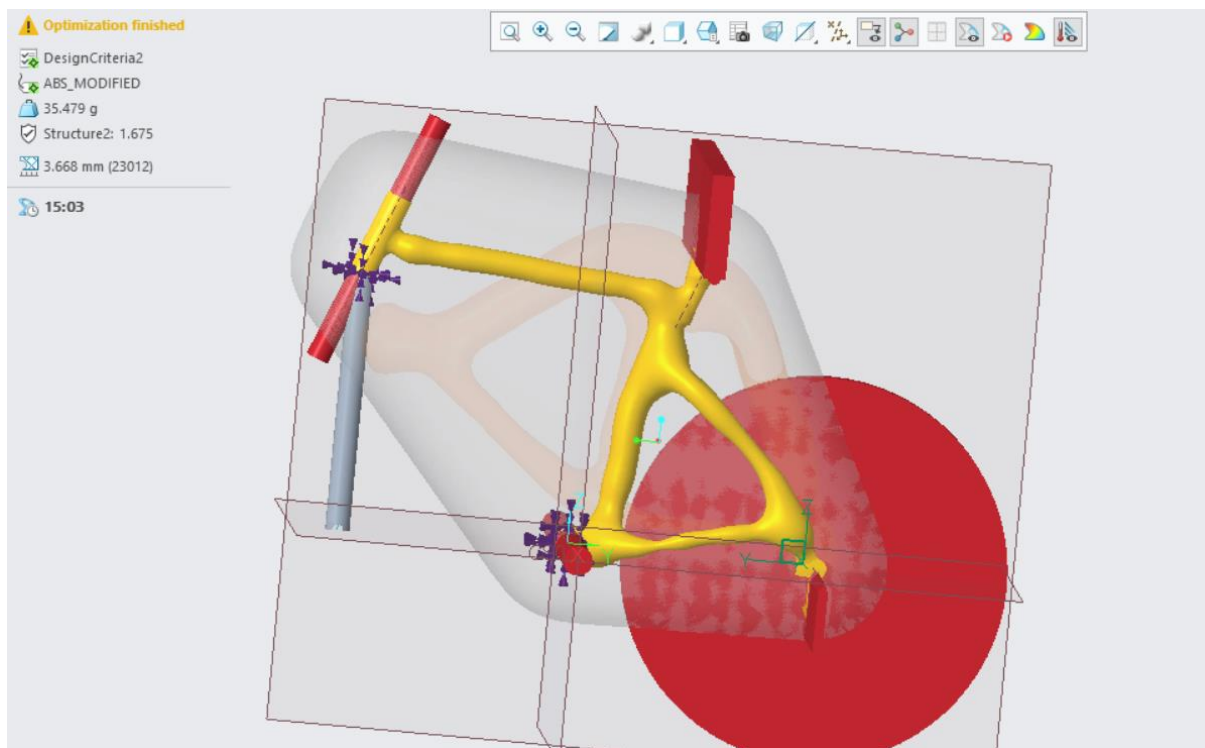
**Figure 33:** Non-converged model with unconventional geometry
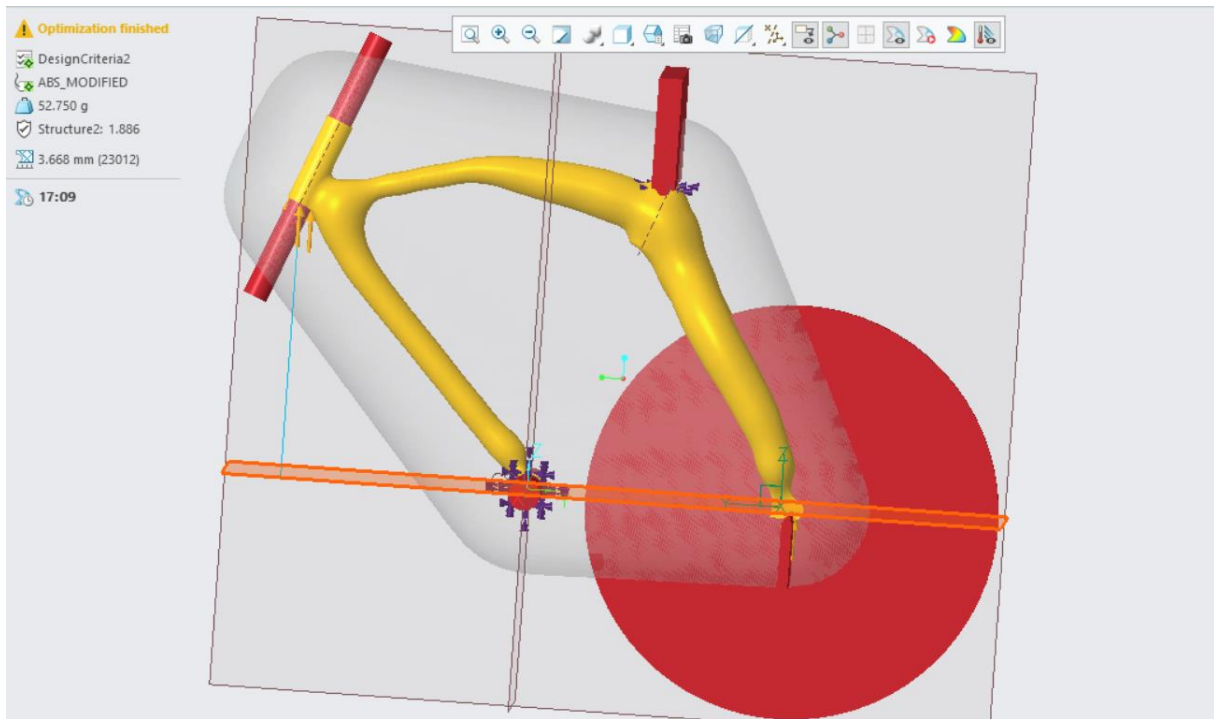
Figure 34: Second non-converged model with lack of connection on the frame
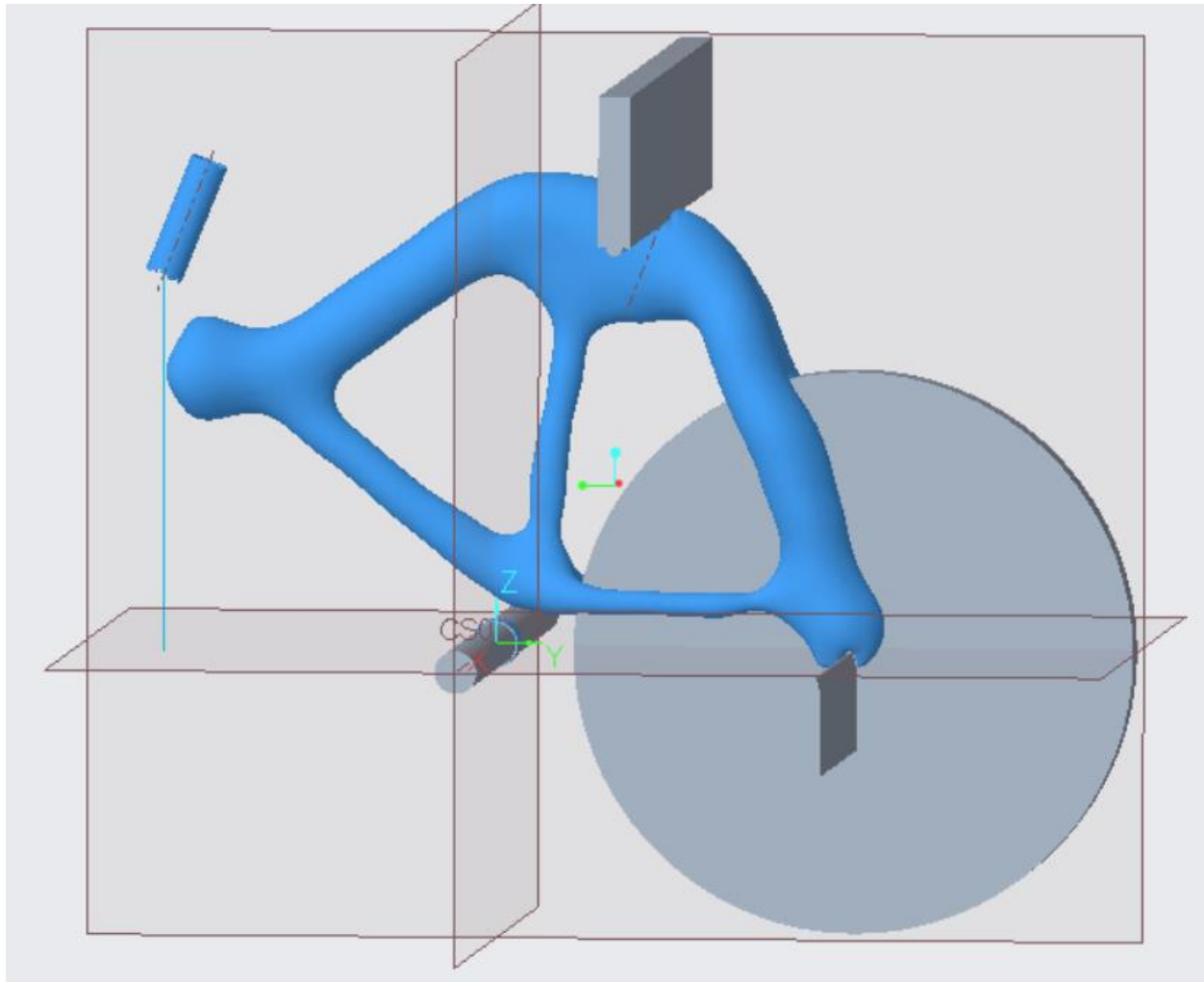
Figure 35: Converged model with no connections to pedals or handlebar

The models only started converging into the general shape of a bicycle frame when the seat location and the pedal connector were fixed. However, the forces were applied at the wheel locations. In terms of testing this, it could be defended as a reasonable frame. The force applied at the seat would have an equal and opposite reaction at the wheel locations. The testing would, therefore, not be ideal since a second fixed point was added to provide extra support for the frame, and the constraints are not a perfect simulation of what would be tested.
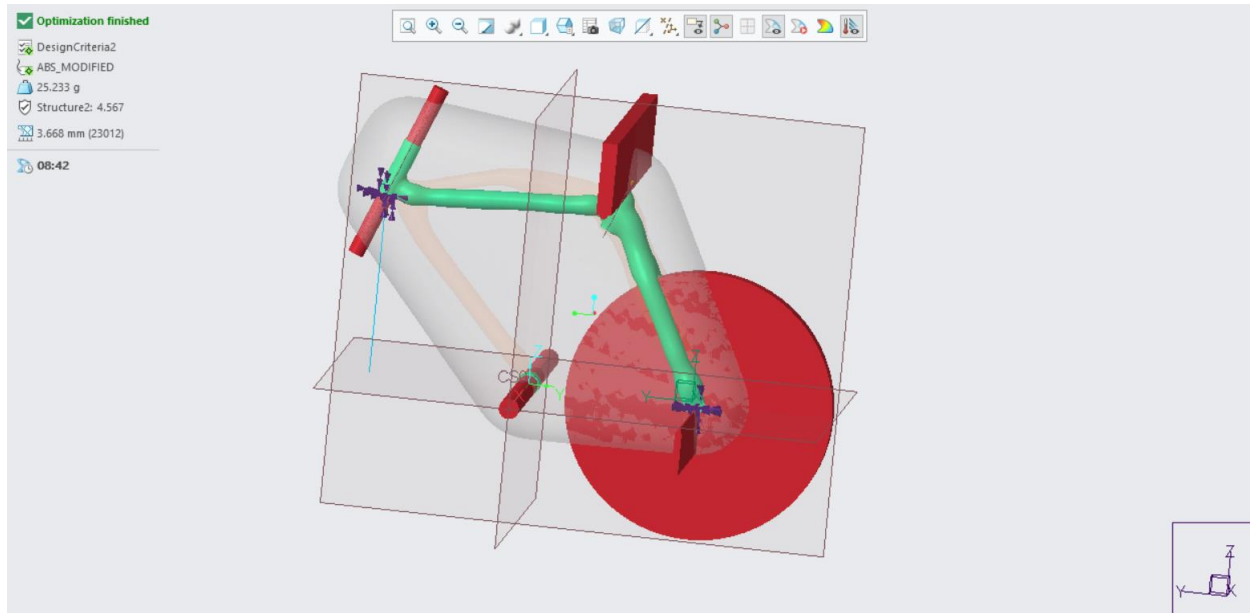
**Figure 36:** Converged model with no connection to the pedals

After testing different reasonable conditions and looking for convergence from the models, some were acquired with forces and even some with applied moments afterward. The force applied to the models was just increased to test what optimized masses the generative design model would return. After looking at all the parts, a total of 12 converged models, after running over 25 different convergence studies, two were selected to test. These two parts were selected since 1) there was no model comparable to the mass of the normal bike frame and 2) they were closely related in the force applied (200N and 250N on each axle), so it would demonstrate how much generative design can do with these small force differences. Note that since the fidelity was only at 3 out of 10, the models have safety factors that are not perfect. More mass could be removed. Increasing the fidelity gives better results which can be seen in a comparison of figures 39 and 40 with figure 48.
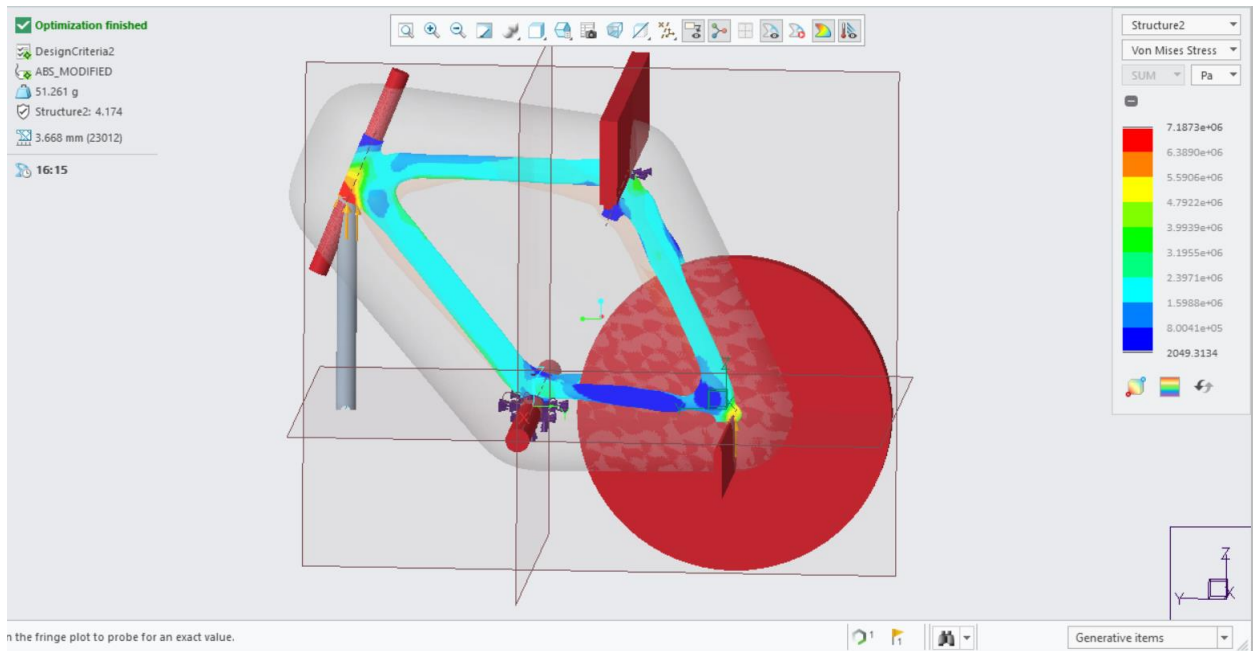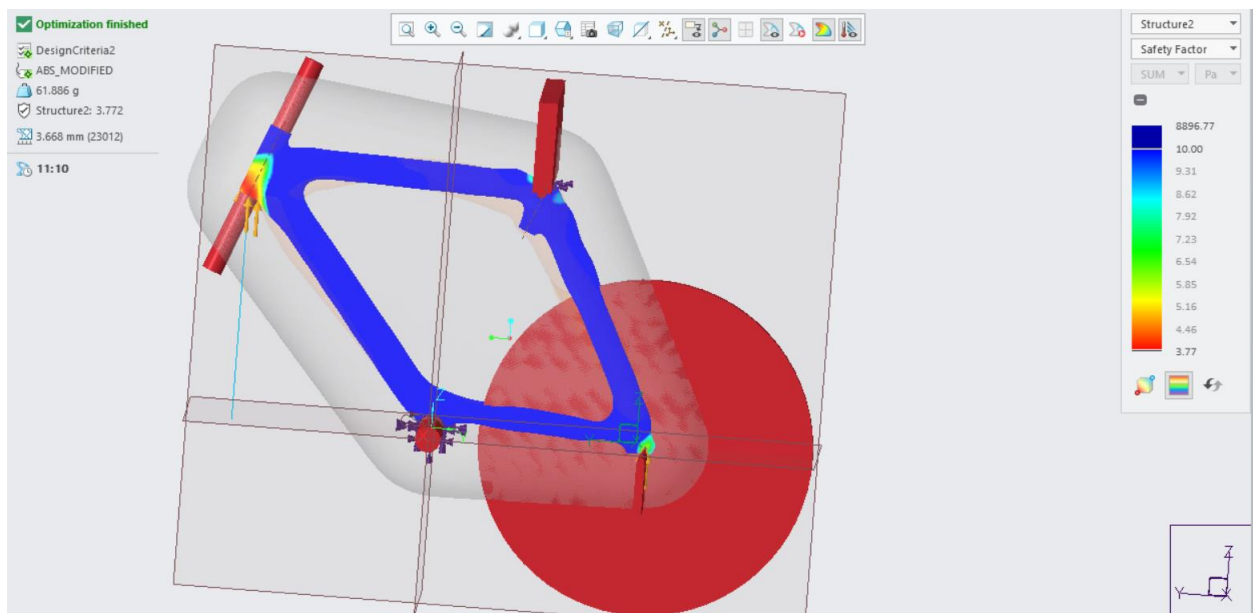
Figure 37: Von Mises Stress for a converged model with 200N on each axle
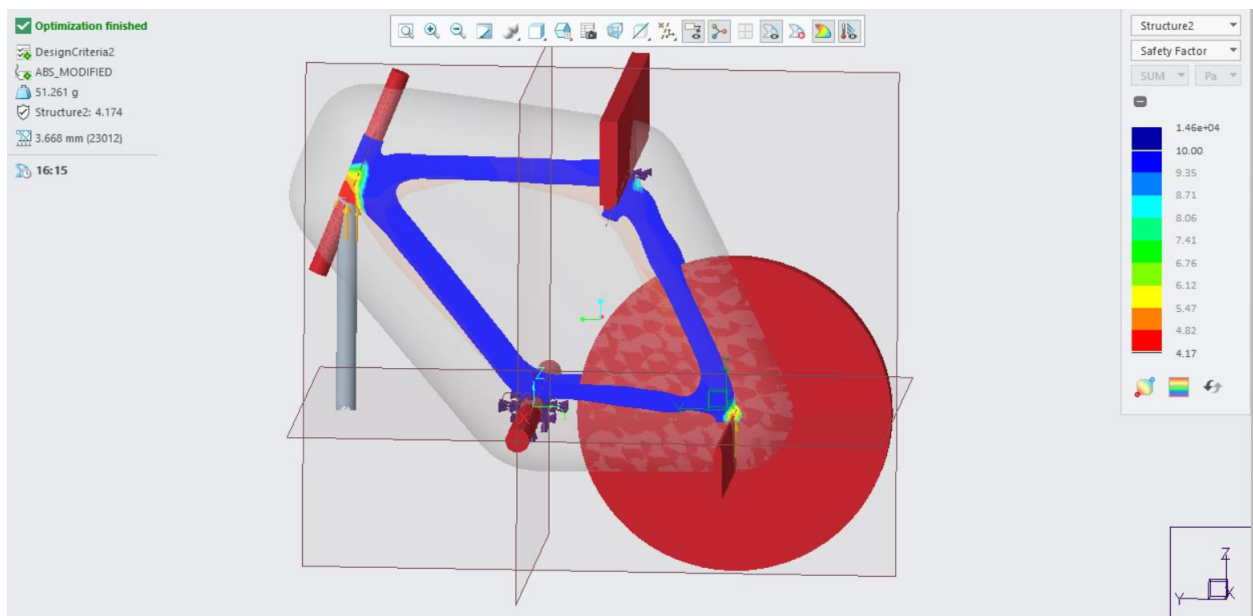
Figure 38: Safety Factor for a converged model with 200N on each axle
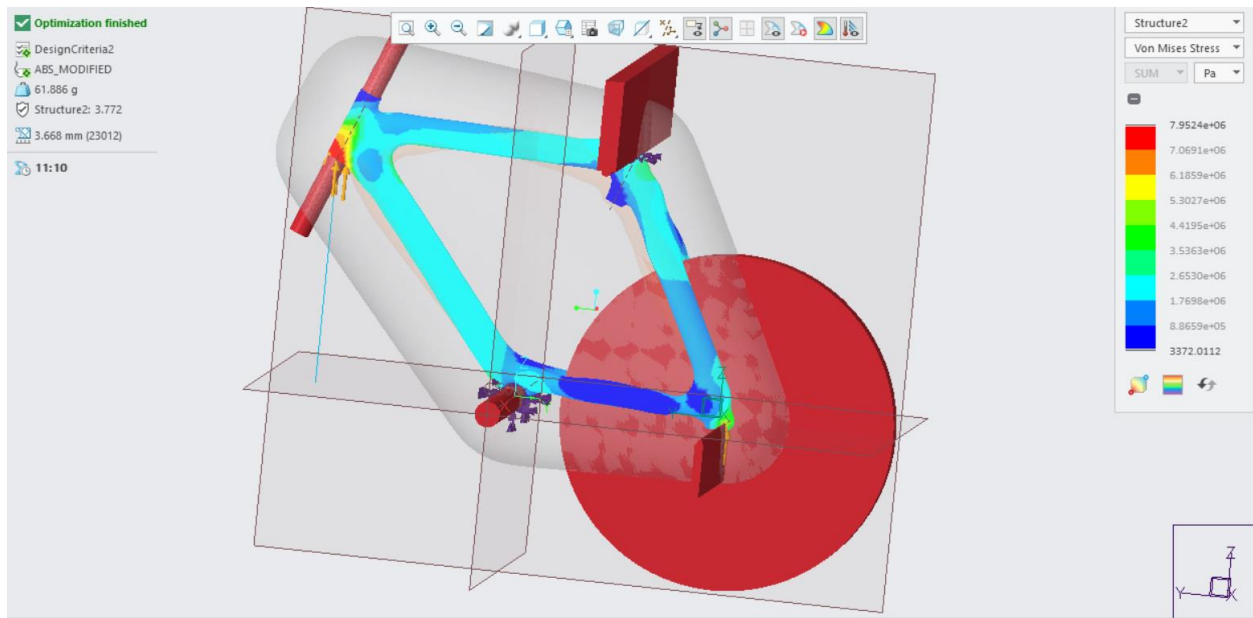
Figure 39: Von Mises Stress for a converged model with 250N on each axle

Figure 40: Safety Factor for a converged model with 250N on each axle

4.2 Model Mass Comparisons

One of the purposes of the investigation was to determine how well generative design would handle optimizing for mass. The generative design was unable to converge for values lower than approximately 120N on each axle using the default study settings. During the process, the material would just be eliminated entirely, and there would be an error pop-up. It is still unclear to me why this happens but it is most likely because the software would attempt to make the connections too thin since it is optimizing based on a factor of safety of 2. If the factor of safety is too large around those parts, it would remove more volume than needed and eventually end up with no more material to work around. However, this was done with the default size of the element sizes. With a more powerful computer, it is possible that forces much lower than this could see convergence by decreasing the size of the element sizes. The number of element sizes could be more than 22 times for this specific study, and the maximum number of iterations almost tripled. In the computer utilized, going to fidelity setting seven would sometimes even take a day.
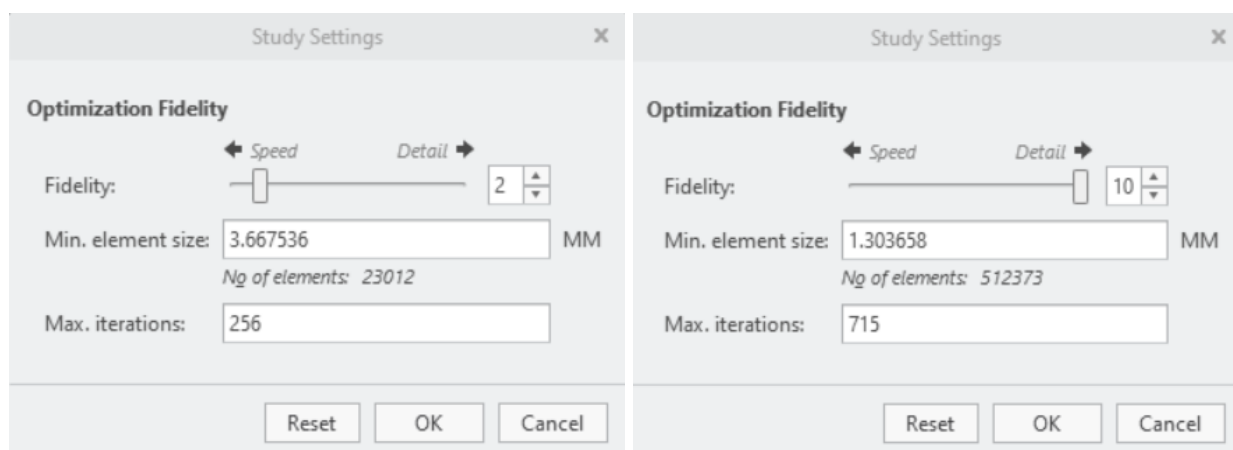

Figures 41-42: The default Creo setting for the Generative study (Left) and the maximum setting possible for the study (Right). The fidelity ranges from 1-10.

By utilizing the masses of the converged studies, which are displayed on the top left of the models, a table and graph could be created to attempt and estimate the mass the model would have for the expected load carried by a normal bike frame and the force a body generated could carry if it had the mass of the original bike frame.

Load Applied at Each Axle (N)	Expected Model Mass (g) Rounded Out
150	40
200	51
250	62
350	75
500	86
650	85
850	97
1000	103

Figure 43: Loads at each axle and mass for the given loads of the converged models
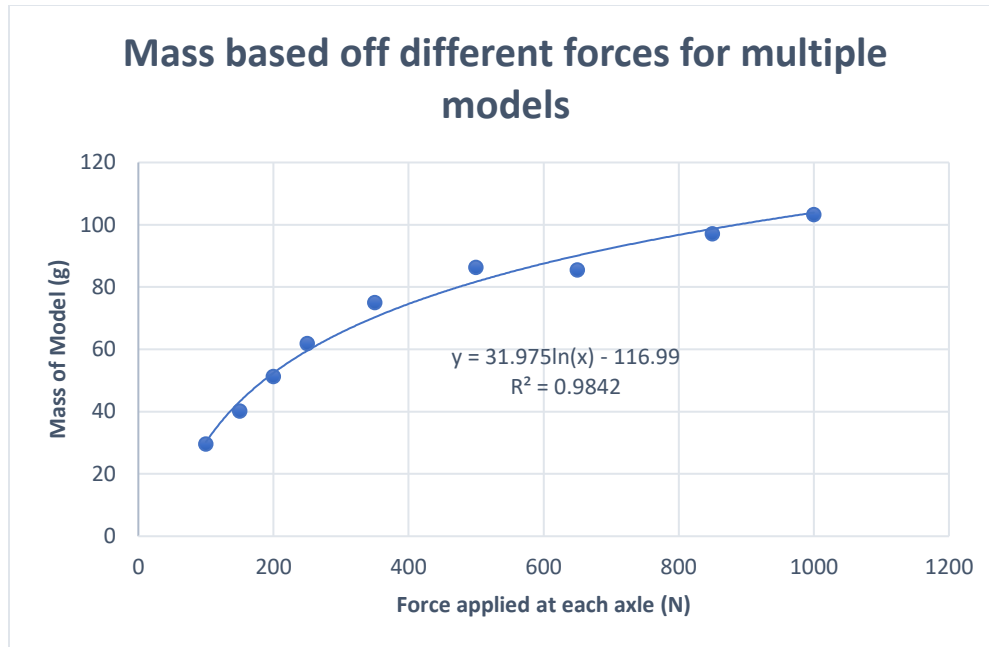
Figure 44: Graph of Table 1 with a logarithmic curve of best fit for the different converged models at different masses.

Upon plotting the acquired data, the logarithmic fit returns an R^2 value of 0.9842 for nine samples with many different forces. It is true that this plot will likely not behave logarithmically at some point for low forces, but if the generative design studies continued this pattern, then at the mass of the original ABS frame (18 grams), the generative design ABS model would hold approximately 67 Newtons at each axle. Considering this is with a factor of safety of 2, then this would be approximately a load of 268N, around 68N more than what was held by the original ABS frame.

4.3 Instron Test Results

The models printed were the frames that were to hold 200N at each axle and 250N at each axle. These were tested in the Instron to test for accuracy. As seen in figures 29-31, the models were not tested in the exact same orientation as in the generative design study but in a

similar position due to how specimens can be studied in an Instron machine. The results indicated the force at failure and displacement of the frame. The stiffness can be seen by the slope of the line.
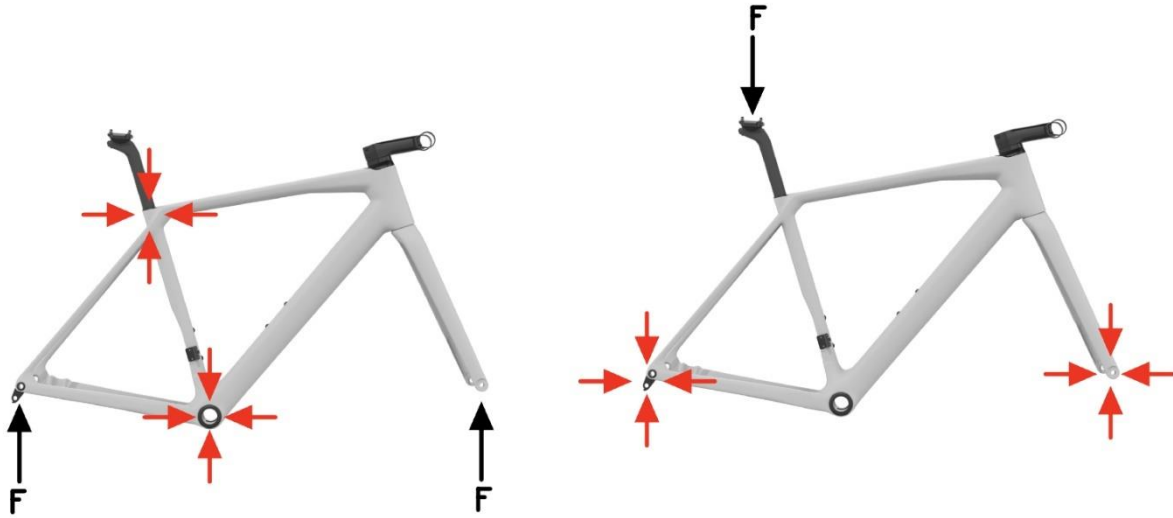
Figure 45: The fixtures (red) and force locations (black) of the generative design study (left) vs. the testing constraints on the Instron machine (right).

The original normal bike frame model was able to hold an approximate load of 200N (205.2N) before failing. The failure location was at the back fork connection with the tube coming from the seat. The other models simulated at 200N and 250N failed at 400N and 683N, respectively. The first is an astonishing result, primarily because with a factor of safety of two, the part should fail at 400N. Another result that was interesting about the part is that it failed not only once but twice at that force. This is a good sign that the optimization is working since a failure at one force multiple times means different components of the part were made to fail at that force. The second part did not quite reach the 800N failure expectation but failed at a factor

of safety of 1.7 instead. The part plastically deforming to 500N after means that the optimization wasn't perfect for the whole bike frame (most likely attributed to fidelity)
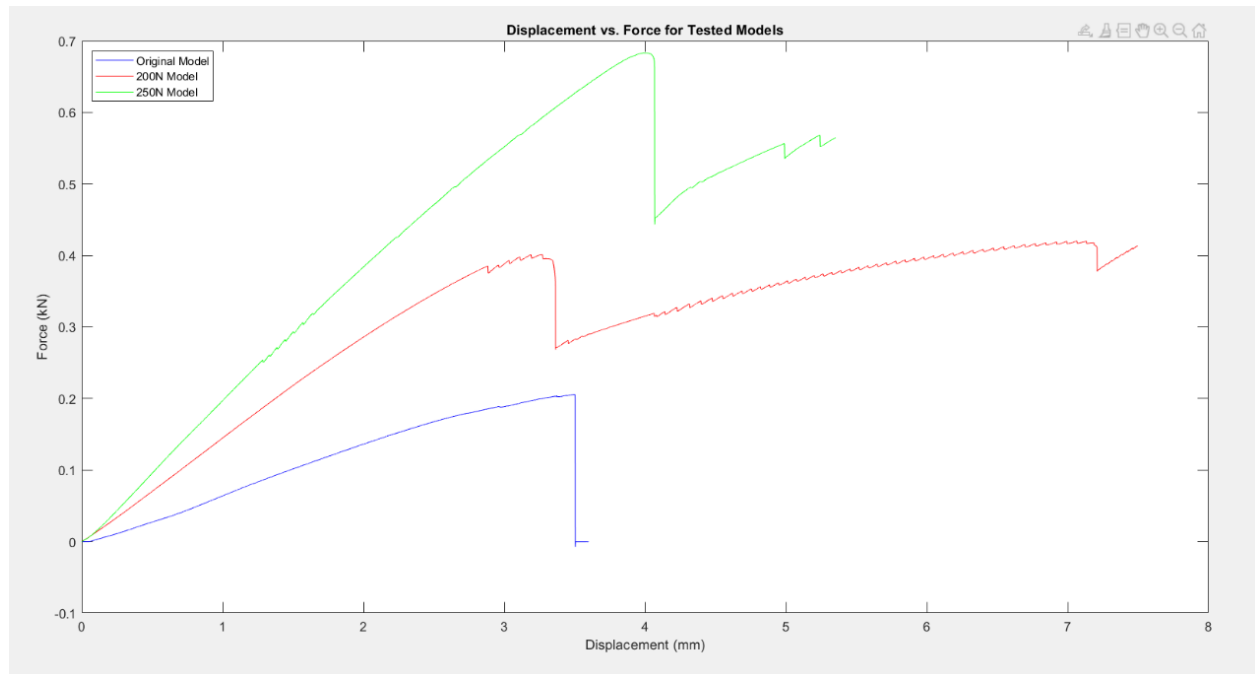

Figure 46: Instron results for the different models: the original frame (Blue), 200N model (Red), and 250N model (green)

At such high forces, imperfections could start becoming a problem. The anisotropy of the material was not taken into account in the models, the 3D printing imperfections and air bubbles between the filament become much more noticeable, and the slight change in orientation between the software constraints and the testing setup also could lead to this 117N difference. In the plot, slight saw-like imperfections can be seen on the curves. This is likely due to the slipping the model experienced in the Test. The model was explicitly not fixed at any location to allow for any deformities to happen (such as bending and displacement), but it did lead to this small noise in the data.

4.4 Attempted Frame Redesign Results

After computing the logarithmic curve of best fit and determining the load on each axle that should have the same mass as the original frame, an attempt was made to increase the fidelity of the study significantly. This did not succeed, and in fact, I was not able to get a frame that was either 1) the same mass but stronger or 2) lighter but could hold the same mass. After generative design studies that took over a day, a 100N on each axle model converged into a frame that showed more features of a model created by generative design.
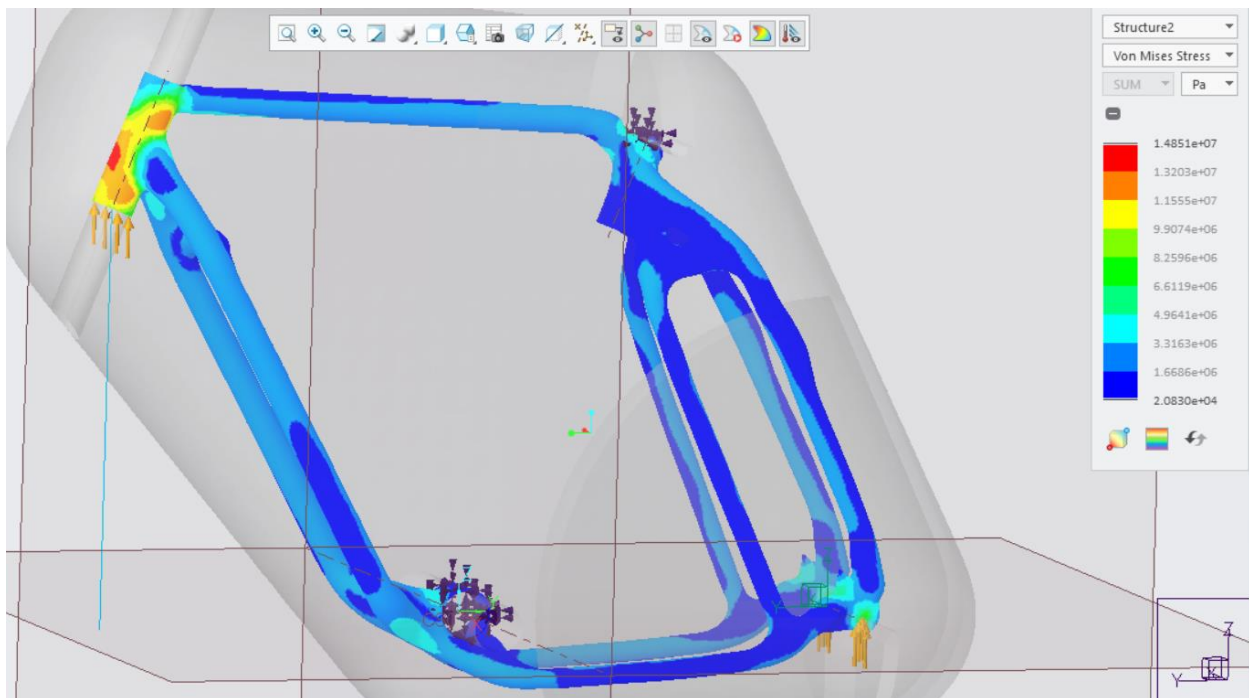
Figure 47: Von Mises Stress for a converged model with 100N on each axle and fidelity 7
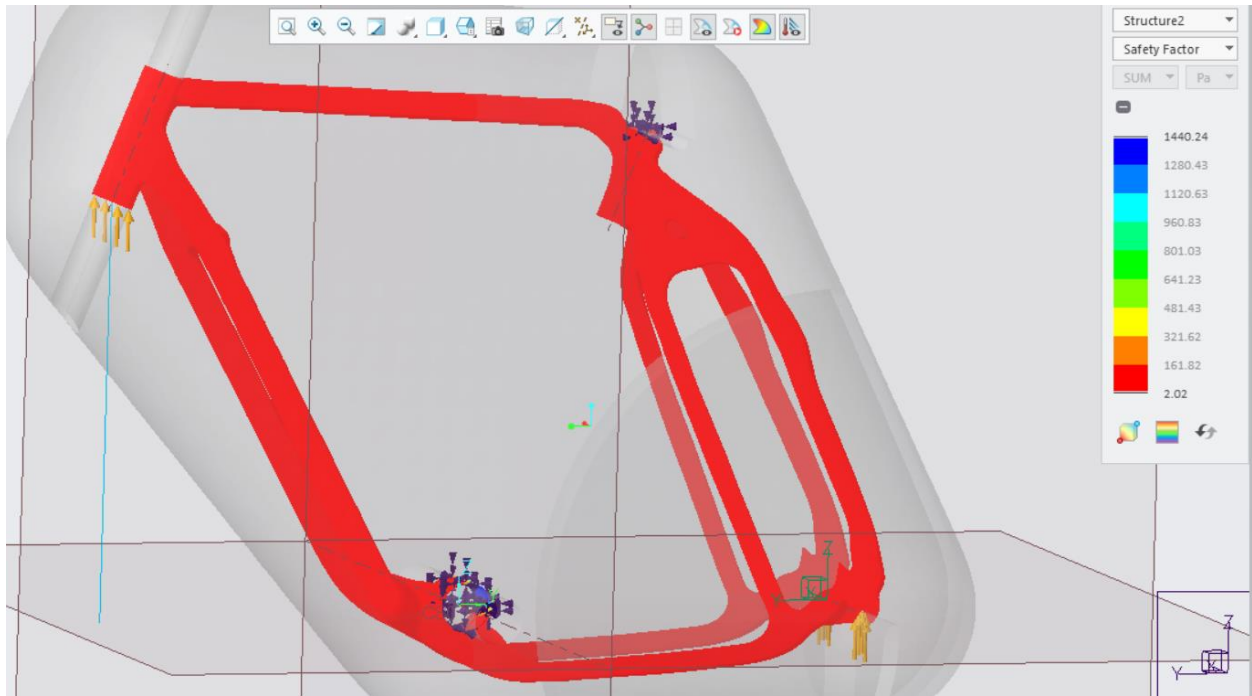
Figure 48: Safety factor for a converged model with 100N on each axle and fidelity 7
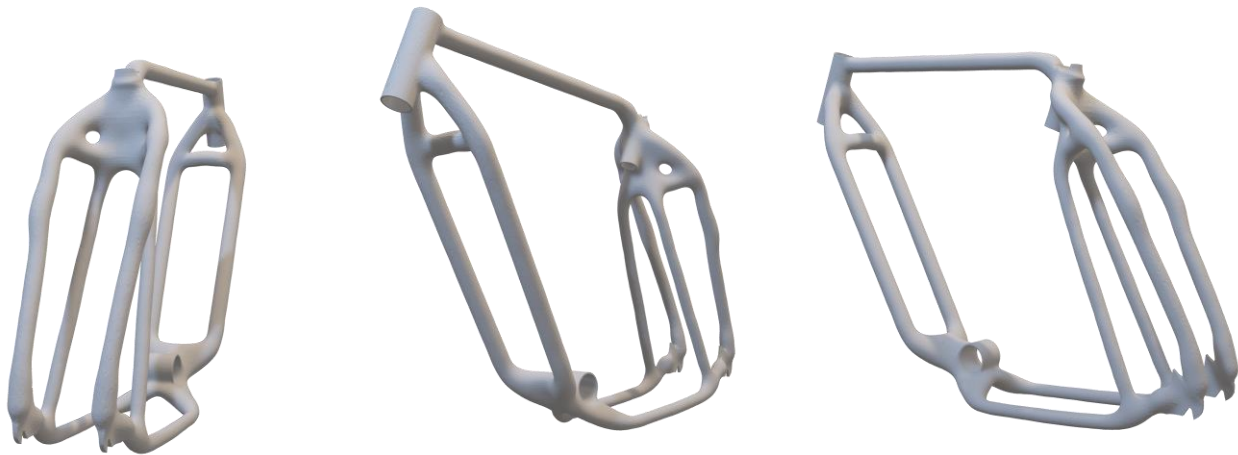
Figure 49: Converged model for 100N on each axle with fidelity level 7

One of my study goals was to get a frame that satisfied the conditions of 1) the same mass but stronger or 2) lighter but could hold the same mass, but after running the studies and determining the study should converge for a force on each axle of approximately 67N, I

determined a fidelity much closer to 10 would be needed, and this would require a much more

powerful computer if fidelity at seven would take over a day to run.
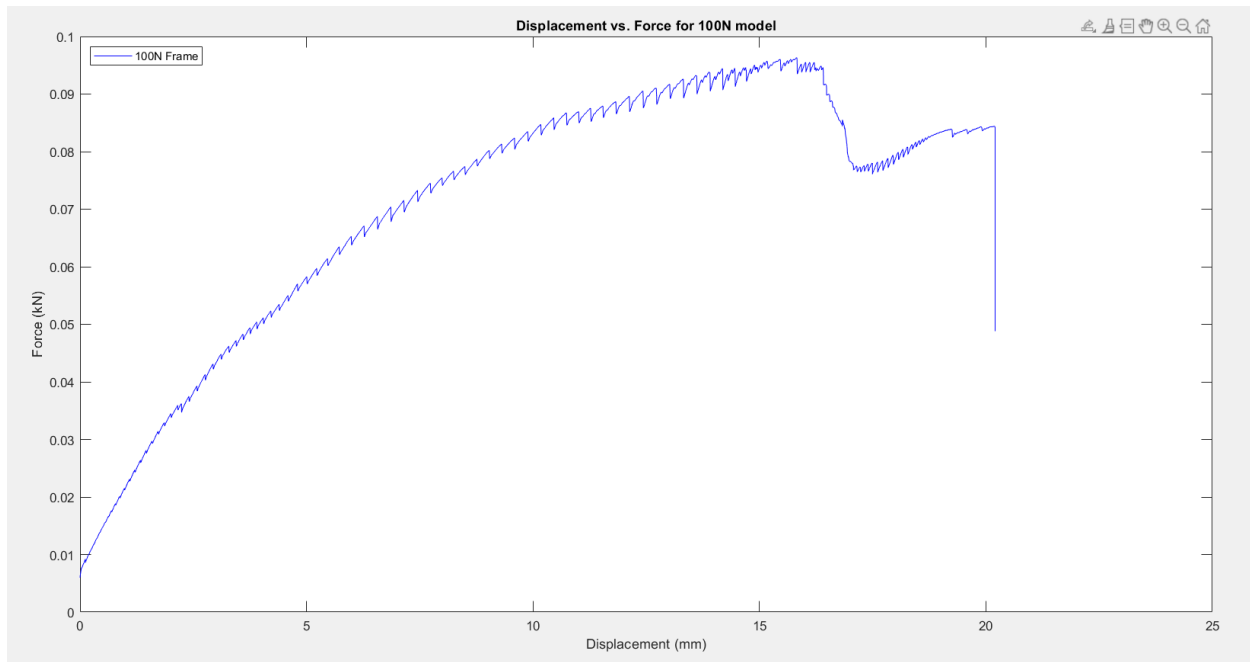
Figure 50: Results for the 100N generative design model at the fidelity level 7, which reached a maximum force of 96.29N before failing.

The results for the fidelity level 7, 100N frame are shown on the plot above (figure 50). The

frame should have been able to hold a load of 200N (considering the safety factor of 2) but failed

at 96.29N. This is a percent error of 51.8% which is significant. This frame, however, was able to

displace over 15mm before failing. This is a lot more than the 3-4 mm from the previous frames.

A summary of the results from all the frames is shown below on figure 51.

Model	Mass (g)	Expected Force (N)	Failure Force (N)	% Error
Original Frame	18	N/A	205	N/A
100N Frame	30	200	96	51.9%
200N Frame	51	400	401	0.25%
250N Frame	62	500	683	36.6%

Figure 51: A table summary of the acquired results from the testing.

Chapter 5: Conclusions

This thesis presented the process of using generative design to change a bike frame. I explored many different boundary conditions to determine which would give the most reasonable results that could be used as an actual bike frame while having a converging study. The frames utilized ultimately were fixed in the two middle points and had to be able to withstand specific forces in the axles. These studies were run on a computer to obtain multiple models that could hold different forces with optimized mass and a factor of safety of two. The models were exported as STL files and printed in a Stratasys F120 with ABS-M30 filament and soluble support SR-30.

The printed parts were set up in an Instron 6800 Model Series (Mid-Range testing system) using the base of a 3-point bend test and a compression plate to apply the force. The parts were set up in a way that allowed for natural displacement and deformation while the Instron machine pressed down on the part and collected displacement and force data. I tested the parts until failure and occasionally more to determine future behavior.

I demonstrated that even with a couple of months of experience with generative design, it is possible to utilize and run studies. I also showed that experimentally, generative design could give accurate results, but the model must be made in a study that is run as close to the real-world application as possible. I also showed that it is possible to fit a curve on a set of studies that can relate the mass between studies for different forces, and this may be possible by optimizing for stiffness as well.

From this work, I concluded that generative design is a very powerful computer software but replicating the real load conditions in the world is extremely hard. The computational power

is also very large, and for more optimized results the element size must be relatively small (at least fidelity level 7). The results agreed to within 1% for one model but were 36.6% and 51.9% off for the other models. Through this work, I was able to show that reliable parts can be achieved through generative design when proper conditions are provided to the software, but may not behave as expected under slightly different conditions.

5.1 Future work

While I was not able to completely meet the goal of designing a bike frame that was lighter, I learned a lot in the process and definitely think it can be done, especially with access to a more powerful computer and fidelity turned all the way to the 10 level. Based on the Instron tests, I have high hopes that the model returned from this process will be highly optimized at those fidelity levels and will hold the loads that are set as the constraints. A printer that can return parts that are isotropic, such as a stereolithography printer, would help polish the results. Otherwise, the exact properties in each X, Y, and Z direction can be inserted for the part in Creo, but since printers alternate in the directions of the layers, they can be hard to find.

In terms of improving the Instron test, a custom setup would have to be made to simulate the studies. The Instron is a machine with one actuator, so a machine with two actuators would be more capable of matching the generative design constraints closely. There are machines that test the fatigue and strength of bikes, so creating one highly detailed frame with generative design and 3D printing it with metal would be a great source of information about the behavior of these parts.

Getting the exact conditions that a frame has to withhold is time-consuming, and running the studies requires a high computational power price. The 3D printing cost is also high for these frames, especially since there are already systems that can mass produce them for cheaper. After going through this process myself, it became clear that this technology is potent but must still be improved and still has some time before it can shape products and make its way into engineering schools.

References

1. Goodacre, Charles J., et al. "CAD/CAM Fabricated Complete Dentures: Concepts and Clinical Methods of Obtaining Required Morphological Data." *The Journal of Prosthetic Dentistry*, vol. 107, no. 1, Jan. 2012, pp. 34–46, https://doi.org/10.1016/s0022-3913(12)60015-8.

2. Ye, Xiuzi, et al. "Today's Students, Tomorrow's Engineers: An Industrial Perspective on CAD Education." *Computer-Aided design*, vol. 36, no. 14, 1 Dec. 2004, pp. 1451–1460, www.sciencedirect.com/science/article/pii/S0010448504000508, https://doi.org/10.1016/j.cad.2003.11.006.

3. "Generative Design Fail: Why Aligning Design Goals and Digital Processes Is Important." *Parametric Monkey*, 26 July 2021, parametricmonkey.com/2021/07/27/generative-design-fail/.

4. Allen, J., and Kouppas, P. "Computer Aided Design: Past, Present, Future" *Design and Designing: A Critical Introduction,* Edition 1, Chapter 7, Jan. 2012 pp. 97-111 https://www.researchgate.net/publication/281455474_Computer_Aided_Design_Past_Present_Future

5. "Here's the Amazing Technology behind the Czinger 21C Hypercar." *Carscoops*, 26 Dec. 2020, www.carscoops.com/2020/12/heres-the-amazing-technology-behind-the-czinger-21c-hypercar/.

6. "Generative Design: What Can It Do for Sustainability?" *Fusion 360 Blog*, 12 Mar. 2019, www.autodesk.com/products/fusion-360/blog/generative-design-sustainability/.

7. Zaraza, Julian, et al. "Generative Design to Reduce Embodied GHG Emissions of High-Rise Buildings." *Automation in Construction*, vol. 139, July 2022, p. 104274, https://doi.org/10.1016/j.autcon.2022.104274.

8. Ziech, Jim, et al. "Design Optimization Method for CAD Structural Components." *SAE Transactions*, vol. 112, 2003, pp. 384–403. *JSTOR*, http://www.jstor.org/stable/44718781.

9. "PTC Help Center." *Support.ptc.com*, support.ptc.com/help/creo/creo_pma/r9.0/usascii/index.html#page/simulate/simulate/struc_loads_top.html#wwID0EK41U.

10. "PTC Help Center." *Support.ptc.com*, support.ptc.com/help/creo/creo_pma/r9.0/usascii/index.html#page/simulate/simulate/constraints_top.html#wwID0EKMGU.

11. Fish, Jonathan, and Stephen Scrivener. "Amplifying the Mind's Eye: Sketching and Visual Cognition." *Leonardo*, vol. 23, no. 1, 1990, pp. 117–26. *JSTOR*, https://doi.org/10.2307/1578475.

12. Bhavikatti, S S, and New Age International (P) Ltd. *Finite Element Analysis*. New Delhi, India, New Age International Pvt, 2015.

13. – S.Tohamy, Ahmed. (2015). Master Thesis. 10.13140/RG.2.1.1955.4409. https://www.researchgate.net/publication/279286495_Master_Thesis

14. University of Cambridge. "Introduction." *Dissemination of IT for the Promotion of Materials Science (DoITPoMS)*, University of Cambridge, www.doitpoms.ac.uk/tlplib/fem/intro.php.

15. Verbart, Alexander. (2015). Topology Optimization with Stress Constraints. 10.13140/RG.2.1.3422.0880. https://www.researchgate.net/publication/286368683_Topology_Optimization_with_Stress_Constraints

16. Prager, W. "Optimization of Structural Design." *Journal of Optimization Theory and Applications*, vol. 6, no. 1, July 1970, pp. 1–21, https://doi.org/10.1007/bf00927037.

17. Yang, Dixiong, et al. "Stress-Constrained Topology Optimization Based on Maximum Stress Measures." *Computers & Structures*, vol. 198, 1 Mar. 2018, pp. 23–39, www.sciencedirect.com/science/article/pii/S0045794917307435, https://doi.org/10.1016/j.compstruc.2018.01.008.

18. Holmberg, Erik, et al. "Stress Constrained Topology Optimization." *Structural and Multidisciplinary Optimization*, vol. 48, no. 1, 1 Feb. 2013, pp. 33–47, https://doi.org/10.1007/s00158-012-0880-7.

19. Gebisa, A W, and H G Lemu. "A Case Study on Topology Optimized Design for Additive Manufacturing." *IOP Conference Series: Materials Science and Engineering*, vol. 276, Dec. 2017, p. 012026, ui.adsabs.harvard.edu/abs/2017MS%26E..276a2026G/abstract, https://doi.org/10.1088/1757-899x/276/1/012026.

20. Zhang, Weihong, and Ying Zhou. "Chapter 6 - Feature-Driven Optimization Method and Applications." *ScienceDirect*, Elsevier, 1 Jan. 2021, www.sciencedirect.com/science/article/pii/B9780128213308000067.

21. "Generative Design in Creo | PTC." *Www.ptc.com*, www.ptc.com/en/technologies/cad/generative-design.

22. "Generative Design 101." *Formlabs*, formlabs.com/blog/generative-design/.

23. – Charles Dapogny, Alexis Faure, Georgios Michailidis, Grégoire Allaire, Agnes Couvelas, et al.. Geometric constraints for shape and topology optimization in architectural design. Computational Mechanics, 2017, 59 (6), pp.933-965. ff10.1007/s00466-017-1383-6ff. ffhal-01354004v3f https://hal.science/hal-01354004/file/S&T_architecture_v5.pdf

24. Pilagatti, Adriano Nicola, et al. "Generative Design and New Designers' Role in the Manufacturing Industry." *Procedia CIRP*, vol. 112, 2022, pp. 364–369, https://doi.org/10.1016/j.procir.2022.09.010.

25. Saeed, Gholizadeh. "16 - Structural Optimization for Frequency Constraints." *ScienceDirect*, Elsevier, 1 Jan. 2013, www.sciencedirect.com/science/article/pii/B9780123983640000164?via%3Dihub.

26. Regenwetter, Lyle, et al. "FRAMED: An AutoML Approach for Structural Performance Prediction of Bicycle Frames." *Computer-Aided design*, vol. 156, Mar. 2023, p. 103446, https://doi.org/10.1016/j.cad.2022.103446.

27. Chung, Chien-Ping, and Ching-Fang Lee. "Parameters Decision on the Product Characteristics of a Bike Frame." *Procedia - Social and Behavioral Sciences*, vol. 40, 2012, pp. 107–115, https://doi.org/10.1016/j.sbspro.2012.03.168.

28. Covill, Derek, et al. "Parametric Finite Element Analysis of Bicycle Frame Geometries." *Procedia Engineering*, vol. 72, 2014, pp. 441–446, www.sciencedirect.com/science/article/pii/S1877705814005931, https://doi.org/10.1016/j.proeng.2014.06.077.

29. "Can a Generatively Designed Bike Please Get Better?" *Engineering.com*, www.engineering.com/story/can-a-generatively-designed-bike-please-get-better.

30. Vanwalleghem, Joachim, et al. "Development of a Multi-Directional Rating Test Method for Bicycle Stiffness." *Procedia Engineering*, vol. 72, 2014, pp. 321–326, https://doi.org/10.1016/j.proeng.2014.06.055.

31. "Decathlon Reimagines Lighter, Stronger, More Sustainable Bicycle Using Autodesk Generative Design." *Autodesk News*, adsknews.autodesk.com/en/news/au-2020-decathlon/.

32. "Mardus | GrabCAD." *Grabcad.com*, grabcad.com/mardus--1.

33. Bergmann, Nathan. *Bike Wheel Size Chart for Height & Age : The Complete Guide*. 5 Jan. 2023, www.bikedenver.org/bike-wheel-size-chart/.

34. *ABS-M30 Data Sheet ABS-M30 FDM Thermoplastic Filament.*
https://www.stratasys.com/siteassets/materials-catalog/fdm-materials/abs-m30/mds_fdm_abs-m30_0921a.pdf

Appendix

1.1 CAD Models

All the CAD models were exported as STL files, named appropriately, and uploaded to OnShape for public viewing/usage

https://cad.onshape.com/documents/2faaae535e703ddd436ede57/w/b0f3cee8746e59d61de696c8/e/0ed49ab7f93f0172c2e9d83b

1.2 Instron Data

The Instron data was uploaded as a zip file to drive and made public. It can be reached with the following link:

https://drive.google.com/file/d/1rgsGhKiaf3MzfaIrLYSg0zt1FsXCQidR/view?usp=share_link